Golder Associates
CONSULTING GEOTECHNICAL AND MINING ENGINEERS

REPORT TO
CANMET

DESIGN, DEVELOPMENT AND MANUFACTURING OF A RUGGED LOAD CELL TO MONITOR AND RECORD LOAD IN LONGWALL WASTES PHASE 1

SYDNEY NOVA SCOTIA

DSS CONTRACT NO. 0SQ84-00161

Distribution:

5 copies - Cape Breton Coal Research Laboratory
Sydney, Nova Scotia

1 copy - Solinst Canada Limited
Burlington, Ontario

1 copy - Golder Associates
Mississauga, Ontario

OCT 23 1985
MICROMEDIA

43 pp

December 1984 841-1251

ABSTRACT

A range of design options have been considered for monitoring the loading from the wastes in a longwall panel. Because of the high load capacity required for the load cell, existing commerically available load cells cannot be directly applied to meet the design requirements.

Four possible load measuring designs were examined, they included: oil filled load cell, displacement load cells, capacitance load cell and measurement of stress changes in the rock mass by means of borehole stress meters. The technology for oil filled load cell has been developed and no major technical difficulties are anticipated in manufacturing a prototype. The technologies for the manufacturing of the components of the displacement and capacitance load cells have also been developed. However, prior to manufacturing a prototype further investigation into the availability of a suitable filler or dielectric material (which exhibit very small long term creep) will be required.

The monitoring of stress changes is technically feasible and should provide a reasonable assessment of the average loading from the wastes.

The use of radio link for transmission of output signals from the instrument is very attractive for the present application, but the development cost is substantially higher than the cable link option.

In order to fulfill the objective of the present study within the budget and time frame for Phase 2 of the research program, it is recommended that the oil filled load cell be manufactured and the field trial be augmented by the stress monitoring scheme.

RESUME

Differentes conceptions ont été considérées regardant la mesure et l'enregistrement des contraintes de chargement causées par l'affaisement de la roche derrière le front d'une exploitation par longue taille. A cause de la grande capacité requise, les capsules de mesure commercialement disponibles ne rencontrent pas les critères de conception pré-établis.

Les concepts suivants furent examinés: capsules manométriques, dynamométriques et di-électriques, et la mesure des variations de contraintes dans le massif au moyen d'indicateurs de contraintes enfoncés dans des trous de forage. La technologie des capsules manométriques existe et aucune difficulté technique n'est anticipée pour la construction d'un prototype. Les technologies requises pour la construction des composantes des capsules dynamométriques et di-électriques ont aussi été développées. Toutefois, avant d'entreprendre la construction de prototypes, des études additionnelles seront nécessaires pour déterminer la disponibilité de matériaux de remplissage et di-électriques adéquats. (très peu de fluage à long terme). La mesure des variations de contraintes est aussi possible et devrait résulter en un estimé raisonnable du chargement moyen causé par la roche effrondrée.

L'utilisation d'ondes radio, pour communiquer avec les instruments situés derrière les étancons, est une option intéressante. Cependant, les coûts de développement sont substanciellement plus élevés que si une liaison par câble était utilisée.

Dans le but de remplir les objectifs de la présente étude à l'intérieur des contraintes budgétaires et temporelles définies pour la phase deux du progamme de recherche, il est recommandé que les essais in-situ soient complémentés par la mesure des variations de contraintes dans le massif, directement sous la zone di'effrondrement.

TABLE OF CONTENTS

	Page No.
ABSTRACT	i
RESUME	ii
1. INTRODUCTION	1
2. BACKGROUND DATA	2
2.1 Objective of the Study	2
2.2 Summary of Visits to Lingan Mine	2
2.3 Available Load Measuring Devices	4
3. DESIGN REQUIREMENTS	6
4. CONCEPTUAL DESIGN OF LOAD CELLS	8
4.1 Design Approaches	8
4.2 Design Alternatives	9
4.2.1 Oil-filled Load Cell	9
4.2.2 Displacement Load Cell	10
4.2.3 Capacitance Pressure Cell	11
4.2.4 Measurement of Stress Changes Below the Floor of the Longwall Panel	13
4.3 Transmission of Output Signals	15
4.3.1 Cable Link Transmission	15
4.3.2 Radio Link Transmission	16
4.4 Field Installation of Load Cells	17
4.5 Calibration of Pressure Cells	18
4.6 Cost Estimate	19
5. CONCLUSIONS	21
ACKNOWLEDGEMENTS	23

LIST OF TABLES

TABLE 1 Commerically Available Load/Pressure Cells
TABLE 2 Summary of Properties of Some Load Sensing Material for Displacement Load Cells
TABLE 3 Vertical Stress Distribution Below A Uniformly Load Strip
TABLE 4 Brief Description of the Function of Radio Link Transmission Components
TABLE 5 Cost Estimate for Radio Link Transmission System
TABLE 6 Summary of Cost Estimates for Load Cells and Stress Monitoring Program

LIST OF FIGURES

1. Configuration of Power Support System at Longwall Coal Face

2. Conceptual Design of Oil Filled Load Cell

3. Conceptual Design of Displacement Load Cell

4. Conceptual Design of Capacitance Load Cell

5. Layout of Borehole for Stress Monitoring

6. Block Diagrams of Probe and Transmission Instrument for Radio Link Transmission

7. Typical Installation of Load Cell

1. INTRODUCTION

Golder Associates, in association with Solinst Canada Ltd., was awarded a contract (DSS Contract No. 0SQ84-00161) by the Department of Supply and Services through the auspices of CANMET to undertake a program of design, development and manufacturing of a rugged load cell to be used to measure loads in longwall wastes.

The project is divided into two phases. Phase 1 entails the conceptual design of the load cells with cost estimates for the proposed options. Phase 2 involves the detailed design and manufacturing of the prototype load cell which is considered by the Scientific Authority to be the most appropriate for the project.

This report summarizes the work completed for Phase 1 of the program and presents several design alternatives that are considered to be feasible from the technical point of view to monitor loads in the wastes. The design principles and limitations, sketches of the main design features and cost estimates are provided for each design alternative. Available output signal transmission and reception technologies and their cost implications are also discussed.

2. BACKGROUND DATA

2.1 Objective of the Study

The success of longwall coal mining depends upon the progressive collapse of the strata above and behind the working face as that face advances through unmined ground. The strata collapse into the mined-out area (gob) which fills with debris and gradually compacts as the mined-out area progressively advances. The characteristics of this compaction within the gob indirectly controls the nature of subsidence development above the worked out areas and in turn, has an important bearing upon the mineability of overlying coal seams and the leakage of groundwater into the workings when the mines are located under surface bodies of water as is frequently the case in the Sydney Coalfield.

For these reasons, the load transferring capability of the collapsed material (wastes) in the gob is of significance in understanding and controlling the development of longwall mining techniques. Very little is known about this phenomenon because of difficulty in obtaining accurate measurements from an area which is hazardous to human entry. The objective of the present investigation is to develop techniques and equipment which will permit the accurate measurement of load distributions below the gob, both in the centre of the area which can be expected to be unaffected by the limits of the excavation, and closer to the roadways where the load sharing effect of the unmined pillars may be expected to play a significant part in the load transfer capabilities of the waste material.

2.2 Summary of Visits to Lingan Mine

With the permission of the Cape Breton Development Corporation (CBDC) and the assistance of Dr. P. Cain of CRL, visits were undertaken in September 1984 by personnel of Golder

Associates and Solinst Canada Ltd. to the Lingan Colliery where longwall advance mining methods are currently being used for coal production. The visits were made to the coal face of the 8E (East) panel whilst mining was in operation. The following is a summary of the observations and data collected during the visits and subsequent discussion with CRL.

The 210 m (700 ft.) longwall face of the 8E panel is currently mined by means of a (DERD) double-drum ranging shearer. At present, the face advance is approximately 18 m (60 ft.) per week, based on 1.8 m per shift and two working shifts daily.

The roof immediately behind the longwall face is supported by a HEMSCHEIDT hydraulically operated self-advancing roof-supports spaced on 1.5 m (5 ft.) centres to provide load (working) carrying capacity of 4.5 MN (500 tons). Figure 1 illustrates the configuration of the powered support system and the shaded area indicates the space between the armoured face conveyor and the base of the roof support system in which the proposed load cell could potentially be installed. The base of the powered support unit would slide over the load cell location as the roof support system is moved forward by hydraulic rams coupled to the face conveyor.

The roof within 7 m (24 ft.) of the waste side of the upper gate road is supported by timber packs spaced at approximately 1.5 m (5 ft.) centres. Beyond the supported area, the roof has collapsed behind the powered support in the mined-out area. The size of the caved material (waste) ranges from 150 mm size fragments to as much as slabs of about 1.5 m across by 0.7 m thick (5 ft. across by 2 ft. thick). The disposition of the fallen debris as observed immediately behind the support units are generally random with a substantial volume of void spaces between the blocks.

The space (approximately 2.0 m wide) between the powered support unit and the armoured face conveyor provides access across the longwall face, but because of the configuration of the support system, it is not possible to use any underground transportation unit to handle material through this area.

2.3 Available Load Measuring Devices

Equipment to measure applied loads is available commercially. Such instruments are conventionally referred to as load cells when the geometry of the applied load is well defined (eg. a rockbolt load cell). When the applied loading of within a medium (eg. soil) or at a boundary (eg. between rock and a tunnel lining), the instruments are termed pressure cells, as this is the parameter of interest.

For this project, in fact, the geometry of the applied loading is not uniform or well defined and, in fact, the pressure applied by the waste to the rock stratum below the mined area is the desired parameters. For the purposes of this report, however, the load measuring devices are referred to as load cells.

Typical commercially available "load cells" are listed in Table 1. Such cells are not directly applicable to this project as they do not provide high enough capacity.

The design principles involved in commercially available cells can however be utilized as the basis for developing the required design. Basically, the "pressure cell" type of design used at the interface between concrete and soil or rock is considered the most appropriate for application to this project. The size, however, would be larger than normal and a higher capacity transducer is required.

Of the commercially available transducer systems, the most common are hydraulic/pneumatic, vibrating wire and electrical strain gauge transducers. For this project, hydraulic/pneumatic design has been rejected as being unsuitable for the following reasons:

- the system cannot be datalogged
- the high pressures to be measured lead to difficulties in reading

Vibrating wire transducers are not manufactured commerically to read 70 MPa (10,000 psi), They could be constructed, but would be expensive to produce because of experimentation, testing and calibration required to produce a good transducer. Electrical strain gauge transducers are available commercially to 70 MPa (10,000 psi). Such transducers are easily datalogged.

The disadvantage of the electrical strain gauge transducer, however, is that this type of transducer has historically been less reliable than vibrating wire transducers, for long term readings (eg. in earth dam applications). Providing that high quality cable is used (this would also be required for vibrating wire transducers), it is considered that this type of transducer would be the most suitable.

3. DESIGN REQUIREMENTS

Based on the observations made of the conditions at the longwall face and the requirements specified by the Scientific Authority, the following is a summary of the design requirements and constraints which are required to be addressed in the design of the load cells.

(a) The only space available for the installation of the load cell is the area between the armoured face conveyor and the powered support units (see Figure 1). This would restrict the maximum dimension (plan) of the load cell to about 0.6 m x 0.6 m (2 ft. x 2 ft.).

(b) The load cell, when in place, would sequentially be subjected to the following loading conditions.

- shearing on the surface of the load cell would take place as the powered support units are being pulled forward by the conveyor during face advance
- bearing pressure would be transmitted to the load cell from the powered support unit when the unit is sitting directly on top of the load cell and providing support to the roof. The maximum pressure could reach 10 MPa
- the load cell would be subjected to impact loading as the roof strata start to cave after the support system has advanced forward. As more materials are caved and compaction starts to take place, static loading would prevail. Nevertheless, the loading pattern on the load cell could be highly unpredictable due to the uncontrolled nature of caving. The load cell may be subjected to point load if the edge of a block landed on the load cell, or not loaded at all due to bridging of the fallen blocks. This type of random loading condition can only be measured by means of a very large (in terms of tens of metres) sensing area or with a large number of load cells of limited dimension. The load cells also have to be adequately protected to resist physical damage under the above loading conditions

(c) Due to the restricted access in front of the powered support, the components of the load cells have to be sufficiently portable to facilitate transportation and installation. From the safety point of view, the installation has to be undertaken under supported areas close to the longwall face. Hence, the installation has to be carried out during weekend periods in order to avoid disruption of the mining activities.

(d) To comply with the Coal Mines (CBDC) Safety Regulations, the components of the load cells have to be intrinsically safe. This includes the load cell itself, and the transmission and readout devices. Once the load cell is in place and caving starts to take place behind the power support, access to the load cells will be lost. It is essential therefore that the load cell be designed as a maintenance-free unit.

(e) A maximum capacity of 70 MPa (10,000 psi) was specified in the Statement of Work for the load cell. A review of the loading mechanism and the depth of the mine indicated that due to the effect of bulking and arching of the wastes, the load to be sustained by the load cell would be substantially less than 70 MPa even when the effect of transient impact loading is taken into account. The maximum pressure is anticipated to be of the order of about 35 MPa (5,000 psi). Further discussions are given in the later sections regarding the implication of the design capacities on the design features and cost of the load cells.

(f) For long term monitoring purposes, the output signals from the load cells have to be transmitted to a permanent readout station located in the adjacent gate roads either by cable or radio link. Considerations would be given to the use of an automated logging system for data acquisition.

4. CONCEPTUAL DESIGN OF LOAD CELLS

4.1 Design Approaches

In developing the conceptual design for the load measuring device in the wastes, the design requirements as discussed in Section 3 were used as the guidelines. In view of the requirements for measuring the overall loading in the wastes, the design effort is directed towards the measurement of the average pressure over the contact area of the load cell. Four design approaches have been considered.

The first is to utilize existing load cell units available commercially. A range of the available load cell and the transducer units has been discussed and summarized in Table 1 in Section 2.3. Minor modifications have to be made to the housing of the units in order to protect the cell from physical damages. This approach could be the most economical option but the maximum capacity of the available load cells is only 27 MPa which is substantially lower than the specified capacity.

The second approach is to build the load cell from basic components. Existing technology including the principles of vibrating wire, linear potentiometers, LVDT's and strain gauges were examined. New transducers and hardware would have to be designed to cater to the specified load capacity requirements. A complete unit might consist of several small load cells wired to produce an average output.

The third approach is to apply other potentially suitable technologies to the load cell design. One possible technology includes the use of a solid filled variable capacitance load cell which incorporates two (or more) plate capacitors separated by a suitable dielectric material. The development costs of such a system would necessarily

be considerably higher than the previous two approaches, but would have the particular advantage that there would be no fluid to leak if the cell was perforated. They are generally rugged and once the initial design is completed and verified would be relatively cheap to reproduce.

The fourth approach is to use the rock mass itself to transmit the load to a sensing element installed in the rock. This includes the measurement of stress changes in the rock due to the loading from the wastes.

The alternative conceptual designs derived on the basis of the above design approaches or a combination of them are described in the following sections. The principles and features of the load cells and the current limitation, if any, of the designs are discussed.

4.2 Design Alternatives

4.2.1 Oil-filled Load Cell

This design utilizes the design principle of oil-filled load cells. The complete unit would consist of two conventional oil-filled load cells with strain gauged transducers rated to measure a maximum pressure of 70 MPa. The load cells can also be wired to a single transducer to provide an average output.

As the oil-filled load cells are susceptible to perforation by point load or impact loading, they are encapsulated in a filler material which is sandwiched between two stainless steel plates. The steel plates provide the surface protection whereas the filler material serves primarily to protect the transducer and cushion the shock due to impact loading. It would also even out the pressure transmitted to the load cells. Synthetic rubber (eg. Neoprene) is

considered to be a suitable filler material. The filler will be bonded to the top and bottom plate to increase the rigidity of the cell. The essential dimensions and features of this design are shown on Figure 2.

The development effort required for the load cell itself is minimal because of the use of conventional units. Electrical strain gauge transducers are available to measure pressures of the required magnitude. Vibrating wire transducers are not available as standard items, although could be manufactured to the specification required.

Some research however has to be carried out regarding the long term creep of the filler material in view of the high design pressure. Further discussions with regard to the creep characteristic of this and similar material will be presented later. Since the material would only be used as a filler, as long as the creep does not cause excessive distortion (flow) of the material, it would not affect the function of the load cell.

4.2.2 Displacement Load Cell

The design principle of the displacement load cell is to measure the displacement of a material of known deformation properties and the average applied pressure is evaluated based on a calibration of the load deformation characteristics of the material. This is in effect a proving ring design. For this application, the width to depth of the proving ring should be high. One mechanical system which was thought to be applicable was the use of very stiff springs. Upon examining the properties of available coiled springs, it was found that the available springs were not strong enough to sustain the design pressure of 70 MPa. This has led to the consideration of other elastic materials such as high density rubber and thermoplastic as the load

sensing material. Based on a study of the properties of these materials, the most suitable material which can withstand the high applied pressure appears to be some type of thermoplastic. The properties of two types of thermoplastic are presented in Table 2. Nylon appears to be more appropriate in terms of its compressive strength.

The displacement load cell basically consists of the sensing material sandwiched between two stainless steel plates which protect the material from physical damage. The displacement between the plates would be measured by means of linear variable differential transformers (LVDT's) or linear potentiometers at several positions to determine the average displacement across the unit. The essential design features of this type of load cell are shown on Figure 3.

Under the maximum pressure of 70 MPa, the elastic compressive strain of Nylon is of the order of about 2%. For a material thickness of 50 mm, the anticipated deformation would be 1 mm. Such displacements are within the measuring capability of LVDT's and linear potentiometers.

However, as all the materials are polymer based, they are also subjected to creep under sustained loading. The creep data in Table 2 suggests that at room temperature and in 1000 hrs., the amount of creep strain could be as much as 50% of the elastic compressive strain in the material. Creep in the longer term is anticipated to be even higher. Such properties are undesirable for the long term performance of the cell.

4.2.3 Capacitance Pressure Cell

This design utilizes the principle of capacitance change in a capacitor to measure the displacement between the plates forming the capacitor. A capacitance pressure cell basically consists of two or more steel plates which would

act as the electrodes for the capacitor. A solid dielectric material would be sandwiched between the steel plates. When the load cell is subjected to the applied pressure, the distance between the steel plates will change due to compression of the dielectric material. This in turn would change the capacitance of the capacitor which is connected to a radio frequency oscillation circuit. The frequency of the oscillations can be read by a frequency counter.

The proposed design comprises three independent capacitors contained in one unit. The layout of the capacitors is shown on Figure 4. The configuration was designed to allow an assessment of load distribution on the unit and to minimize non-uniform displacement across the electrodes. The central portion of the unit was designed to house the frequency oscillators and the transmitter for the output signal. Three electrodes are used for the capacitor, the top and bottom plates are necessary protection to the unit, the central plate can be a thin plate as it is adequately protected. The edge of the cell would be sealed with a 'C' shaped edge piece such that the compression of the dielectric material would not be inhibited.

The dielectric material can be selected from a range of materials which are non-conductive, have good dielectric properties, and are of sufficient strength to sustain the applied pressure. The materials listed in Table 2 appears to suite these requirements, but the creep characteristics inherent in these materials would again affect the long term performance of the cell. Further investigation into the availability of a suitable dielectric material is required prior to detailed design of the prototype.

4.2.4 Measurement of Stress Changes Below the Floor of the Longwall Panel

Apart from the direct method of measuring the loads in the wastes itself, the rock mass could be used as a medium to transmit the loading from the wastes to a sensing instrument installed in the rock mass below the floor of the mined out area. In connection with this concept, the vertical stress distribution below the floor of the mined-out area was examined. Table 3 presents the vertical stress at different depths and distances from the centreline of the extracted longwall panel as a function of the pressure applied on the floor of the panel. It may be noted that if 2b = 200 m (width of the longwall panel), the vertical stress within 20 m of the floor and 50 m of the centreline of the panel would be about 98% to 100% of the applied vertical pressure. Hence, if a sensing element is installed within this zone the measured stress changes would closely reflect the average applied loading from the wastes.

One type of instrument that can be applied to monitor the stress changes includes the Irad Gage vibrating wire stress meter. This instrument consists of a hollow steel cylinder which (when in use) is preloaded diametrically across the sides of a 38 mm dia. (E size) boreholes by means of a sliding wedge and platen assembly. Stress changes in the vicinity of the borehole would cause diametral deformation of the borehole which is sensed by the stress meter. By calibration, the instrument readings are related to stress changes in the rock for a range of rock types. Installations of 15 to 20 m depth have been very common for this type of instrument, but installation of up to 90 m has also been undertaken.

This monitoring scheme involves the drilling of a 38 mm dia. hole from the gate road into the unmined area of the longwall panel. The hole would be drilled downwardly inclined at the orientation and to the depth shown on Figure 5.

Because of the extensive loading area of the longwall panel as discussed above and the shallow inclination of the borehole, the instrument, if installed with the platen in the vertical plane, would be able to measure the vertical stress changes in the rock mass. The inclination of the borehole would only cause an error of about 1% in the measured vertical stress component.

To monitor the loading at various distances from the centre of the longwall panel, three stress meters would be installed in the same borehole at different depths as shown on Figure 5. This procedure, however, requires careful installation techniques. Otherwise, separate holes of different lengths can be drilled for convenience of installation. The installation can be repeated if more than one instrumentation station is desired. Because of the depth of installation, the hydraulic installation tool would be required.

Drilling of long E size hole requires good control and the use of a suitable underground drill. The 42 m long E size hole between tunnel No. 2 and 3 for insitu modulus testing at Donkin was drilled using a Longyear 38 underground drill. The maximum deviation was only about 150 mm from the target position. Hence, significant alignment deviation is not anticipated provided the hole is carefully drilled. The final alignment of the borehole can also be checked with a borehole orientation device if required. To avoid disruption to the mining operation, drilling may have to be undertaken during a weekend period.

One factor which would affect the interpretation of the results is the modulus of the rock mass in which the instrument is installed. The intact modulus from biaxial tests on overcored sandstone and siltstone samples from No. 26 Colliery ranges from 13 to 35 GPa. The insitu modulus of the rock mass in the vicinity of the floor is anticipated to be of the order of 7 GPa or lower. At this low modulus range, the effect of rock modulus on the measured stress changes would become insignificant.

The primary concern with regard to this instrumentation is related to the susceptibility of damage to the instrument cable caused by excessive differential displacement of the rock strata such as floor heaving as observed in some areas of the gate road visited. Some degree of protection may be provided by drilling the first 30 m of the hole to A size (48 mm dia.). This section would be lined with EW casing (46 mm dia. O.D., 38.1 mm dia. I.D.) to contain the instrument cable.

The main advantage of this type of monitoring scheme is that the instrument could be installed prior to mining and there is no requirement to gain access to the operating longwall face. The problem of point loading which confronts most direct measurement by contact load cells would also be eliminated because such effect will be averaged out as the vertical stresses are transmitted through the rock mass to the sensing instrument.

4.3 Transmission of Output Signals

Regardless of the type of device used for measuring the loads in the wastes, the output signals from the instruments have to be transmitted to the readout station for data acquisition. Two types of output signal transmission were considered. The first is the conventional transmission procedure using electrical cables directly led out from the instrument. The second is the radio transmission method which utilizes radio signals to activate the transmission and reception of data. In both methods, the conditions under which the transmission link has to function have necessitated the use of special protections and precautionary measures. The proposed procedure and mode of operation for each of the method of output signal transmission are presented below.

4.3.1 Cable Link Transmission

The length of cable transmission depends on the location of the load cells. With a longwall panel of 200 m in width,

the maximum cable length across the panel would be about 100 m. Because of the configurations of the powered support units (see Figure 1), and the way these support are advanced, any cable link across the longwall face would be susceptible to damage by the mining activities unless the cable is adequately protected.

This would entail the use of a small diameter armoured steel cable (such as Datatrans from Canada Wire and Cable) which is designed to withstand considerable bending and twisting. Despite this provision, the cable has to be placed in cable conduits buried below the floor level of the panel to avoid the risk of shearing the cable as the powered supports are pulled forward. Due to the confined space in front of the powered supports and the time constraints, this procedure could be very labour intensive. After the cable is led into the gate road, it can then be wired to switching units for manual or automic data acquisition. The cost associated with this system of transmission is the cost of the cable link.

4.3.2 Radio Link Transmission

Radio link transmission provides an alternative method of communication between the instruments and the readout options. The radio link replaces the conductor inherent in cable link and allows mobility over distances within certain limits depending on the transmitter power, antenna propagation properties and receiver sensitivity. The communication range is greatly affected by the medium between the receiving and transmitting antenna. The lower frequencies (100 kHz range) are generally used for underground communication. Based on the report on "Research and Development Contract for Coal Mine Communication System" (USBM Report contract No. HO232056), reliable communication can be achieved up to about 70 - 150 m. Under adverse conditions where the load cell is submerged (due to ponding of water at the location where the load cell is installed), the use of wire rope cable loosely coupled to the cell would enhance the propagation of radio signals.

The radio link transmission system comprises two components, the probe and the transmission instrument. The probe is a built-in component of the load cell which utilizes the radio link for data transmission. The transmission instrument activates the transmission of the data. The block diagrams presented on Figure 6 illustrate the essential components which make up the probe and the transmission instrumentation, and the basic logic of their functions. Brief descriptions of the functions of each of the components are presented in Table 4. A brief outline of the mode of operation of the transmission systems is given below.

The probe can be preprogrammed to transmit data at specified time intervals or activated manually from the transmission instrument. In the manual operation mode, the operator would come close to the load cell location, dial the address of the selected probe and press the 'activate' button on the transmission instrument. The transmitter in the instrument will then send pulse coded signals to the specified probe. The addressed probe, originally in low power consumption receiving mode will turn the measurement circuitry on, perform the measurement, store the data and prepare for transmission. The transmitter circuitry is then activated and data is transmitted to the instrument where it is received, decoded and displayed or processed. It can be recorded on magnetic tape for subsequent processing in the laboratory.

The estimated costs associated with the development of a prototype circuit and the manufacturing of a production unit for radio link transmission is presented in Table 5.

4.4 Field Installation of Load Cells

With the exception of the stress monitoring using stress meters, all the load cells require installation close to the coal face immediately in front of the powered supports. The space available for the load cell is shown on Figure 1.

The maximum dimensions of the load cells were designed to fit within this area. In order to avoid disruption of the mining operation, installation of the load cell has to be undertaken during a weekend period where there is no mining activity.

The installation procedure is common to all load cells because they are designed as self-contained unit which can be directly placed at the desired location. The major task in the installation procedure is to ensure that the load cell is adequately protected under the different loading conditions as described in Section 3.

A typical installation is illustrated on Figure 7. The floor is generally excavated to a depth of 0.3 m by means of mechanical equipment (such as jack hammer) over the area where the cell would be placed. A screed of high strength quick set cement grout would be laid in the excavated area to provide a level bedding for the cell. The cell can be temporarily supported and levelled with small cement blocks while the grout sets. The remaining space is then back-filled with sand and a steel plate placed over the sand fill such that it is level with the floor.

If a cable link is used for signal transmission, the excavation of the cable trench has to be undertaken at the same time.

Steel pipe is recommended for the cable conduit and the cable trench should be backfilled with concrete.

4.5 Calibration of Pressure Cells

Each load cell has to be calibrated prior to installation. Two aspects have to be addressed in the calibration program. The first is static calibration where static loading is

applied to the load cell up to the maximum capacity. The effect of eccentric loading would be studied. The loads will also be cycled to examine the loading and unloading characteristics of the cell.

The second is the aspect of impact loading. The load cell would be subjected to impact loads to simulate the possible insitu loading conditions. The magnitude of the impact load would be equivalent to the weight of a slab of rock falling over a distance of about the height of the longwall panel. As the size of the caved material is highly variable a range of loads would be tested.

4.6 Cost Estimate

This section provides a summary of the estimated cost for each of the design options discussed in Section 4.2.

(a) Cost of Hardware for the Load Cell.

This comprises the necessary component for the complete load cell unit. In the case of the stress monitoring scheme, this would include the cost of the stress meter and the drilling costs.

(b) Cost of Installation.

This includes the manpower and equipment cost associated with the installation of the load measuring devices. A labour rate of $50/hr. was assumed for all personnel involved in installation. A total of about 180 man-hours were allowed in the cost estimate for installation of the cell and laying of the cable link.

(c) Cost of Output Data Transmission.

This includes the cost for transmitting the output from the load measuring device to the readout station by both the cable and radio link as described in Section 4.3. For the purpose of comparison, the readout

station is assumed to be located in the gate road at about 10 m back from the face position where the load cells are installed. Costs of switching and readout units are also included.

(d) Cost of Calibration

This includes the manpower and equipment costs for calibrating the load cells for different loading conditions as described in Section 4.5.

A summary of the cost components for each of the design options is presented in Table 6. The approximate time required for manufacturing one unit of each of the proposed design options is also included.

As far as the budgetting for Phase 2 of the program is concerned, the cost of hardware, output data transmission and calibration are the only relevant cost items, the cost of installation is presented for future reference only.

5. CONCLUSIONS

A range of design options have been considered for monitoring the loading from the wastes in a longwall panel. Because of the high load capacity required for the load cell, existing load cells available commercially cannot be directly applied to meet the design requirements. Four possible load measuring designs were examined. They included:

(a) Oil-filled load cell comprising of high capacity oil filled load cell units encapsulated in a filler material and protected by stainless steel plates.

(b) Displacement load cell consisting of a compressible material sandwiched between two protective steel plates. Displacements are measured by means of LVDT's or linear potentiometers and pressures are evaluated from the calibration of the pressure deformation characteristics.

(c) Capacitance load cell, which comprises three separate capacitors each of which comprises three electrodes separated by a solid dielectric material.

(d) Measurement of stress changes in the rock mass by means of a sensing instrument installed below the floor of the longwall panel.

The cost summary in Table 6 provides an approximate cost comparison of these design options.

The technology for the oil-filled load cell has been fully developed and no major technical difficulties are anticipated in manufacturing a prototype load cell.

As far as the displacement and capacitance load cells are concerned, most of the components for the load cells are available or the technologies for the manufacturing of

these components have been developed. The capacitance load cells would be cheap to produce once the initial design is completed and verified. The difficulties however are related to the intrinsic creep characteristics of polymer based materials which appear to fulfill most of the other design requirements. At present, it is not possible to manufacture a prototype without further investigation into the availability of a suitable filler or dielectric material which would only exhibit very small long term creep under high sustained loading.

The monitoring of stress changes is technically feasible and should provide a reasonable assessment of the average loading from the wastes.

In order to fulfill the objective of the present study within the budget and time frame for Phase 2 of the research program, it is recommended that the oil-filled load cell be manufactured and the field trial be augmented by the stress monitoring scheme outlined in (d). The concept of a capacitance load cell is promising but would require further work prior to the development of a prototype unit.

The use of radio link for transmission of output signal from the instrument is particularly attractive for the present application, but the development cost far exceeds the budget available for manufacturing the load cells. The cable link transmission is considerably cheaper but is susceptible to physical damage and therefore requires adequate protection as described in Section 4.3.1. Due to the configuration of the powered support units at the face, installation of the cable link transmission from the instruments to the readout station would be very labour intensive. As such, the manpower requirements for the installation of the load cell have to be examined closely to determine the feasibility of completing the installation during a weekend period. Otherwise, the trial positions may have to be brought closer to the gate road to reduce the length of cable trenching.

Acknowledgements

Golder Associates wishes to thank Solinst Canada Ltd. for their contributions to the project and the helpful suggestions of Dr. P. Cain during the technical review of the draft report.

GOLDER ASSOCIATES

C.M.K. Yuen, P. Eng.

for J.M. Boyd, P. Eng.

CMKY/JMB/dh

TABLE 1 COMMERCIALLY AVAILABLE LOAD/PRESSURE CELLS

MANUFACTURER	TYPE OF LOAD CELL MODEL	DIMENSIONS	CAPACITY	SENSITIVITY	REMARKS
Slope Indicator (Terrametrics)	CC-600 Strain Gauge	diameter = 250 mm height = 150 mm weight = 42 kg.	600T 6.9 MPa	0 - 2 %	Constructed from high strength steel elements to which several sets of matched strain gauges are bonded. Note: multiple strain gauges ensures an accurate response to off-centre loads
	CPC Hydraulic Borehole Cell	diameter = 38 mm (EX) weight = 250 mm height = 2.3 kg	27.5 MPa	69-170 kPa (depending on gauge)	Borehole depth up to 15 m
	BPC	diameter = 250 mm & 63 mm weight = 2.3 kg.	27.5 MPa	69-170 kPa (depending on gauge)	Flatjack type. Borehole depth up to 15 m. This is a flatjack load cell designed to be grouted inside a 64 mm ø borehole. Unlike the CPC, which reacts equally to pressure from any direction, the BPC will respond only to pressure changes in the direction penpendicular to the plane of the flatjack. Note: larger flatjacks for use in flat slot are available on reques
	Total Pressure Cell 51482	diameter = 230 mm thickness = 11 mm weight = 3.6 kg.	2 MPa	0.1% to 0.25% (depending on gauge)	Flatjack type filled with antifreeze Higher capacity ranges available on request

(cont'd...)

TABLE 1 (cont'd)

MANUFACTURER	TYPE OF LOAD CELL MODEL	DIMENSIONS	CAPACITY	SENSITIVITY	REMARKS	TRANSMITTER TYPE
Roctest	Total Pressure Cell B40/40 M300	up to 400 mm by 400 mm	up to 27.5 MPa	± 0.01 MPa	Flatjack Type Oil or mercury filled	Hydraulic/ Pneumatic
Irad Gage	VW Total Pressure Cell EPC-1000	diameter = 9 inch	6.9 kPa	6.9 kPa	Flatjack Type Oil or mercury filled	Vibrating Wire
Soil Instruments Ltd.	1P series	152 mm diaphragm	0.7-2.5 MPa	less than 1% of full load	Vibrating wire strain gauge anchored parallel to level of the two diaphragm availabe for measurement of pressure at interface of concrete and soil/rock	Vibrating Wire
	3P series	low pressure 105 mm to 270 mm dia. high pressure dia. 115 mm to 200 mm x 300 mm	low pressure 0-3.5 MPa high pressure 0-20 MPa	± 1% full scale	oil & mercury filled available for measurement at interface of concrete and soil/rock	Hydraulic/ Pneumatic
	6P series	low pressure as per 3P series high pressure as per 3P series	low pressure 0-5 MPa high pressure 0-20 MPa	± 0.1% full scale	oil & mercury filled available for measurement at interface of concrete and soil/rock	Vibrating Wire Electrical Strain Gauge also available

TABLE 2 SUMMARY OF PROPERTIES OF SOME LOAD SENSING MATERIAL FOR DISPLACEMENT LOAD CELLS

Type of Material	Supplier	S.G.	Modulus of Elasticity	Compressive Strength	Creep Properties
Hytrel 7246	Dupont	1.25	(0°C) 400MPa (20°C) 350MPa	0°C, 75MPa, 25% strain 20°C, 65MPa, 25% strain	.5% (a)
Nylon (1) general information	-	1.14 1.16	not quoted	965-1100MPa	not quoted
(2) vekton 6SA	Ertalon	1.14	(73°F) 1275MPa	48.9MPa (shear strength @73°F)	not quoted
(3) Nylon 6/6 33% glass fibres reinforced (b)	-	not quoted	not quoted	202.7MPa	@70 MPa (10,000 psi) creep modulus after 1hr =9721MPa after 100hr =6101MPa (c)

(a) Compressive creep strain in % for a load of 6.9MPa @ 23°C - creep strain= $\frac{\text{stress}}{\text{creep modulus}}$

(b) Glass fibre direction affects properties

(c) Calculated from total creep strain or deflection before rupture and onset of yielding

Golder Associates

TABLE 3

VERTICAL STRESS DISTRIBUTION BELOW
A UNIFORMLY LOAD STRIP

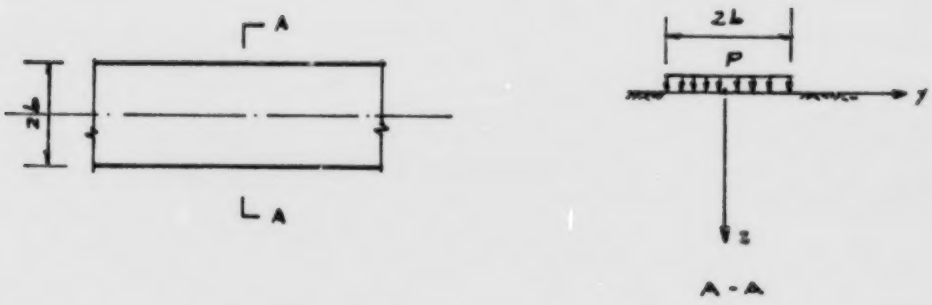

Length of strip = assumed to be infinite
2b = width of strip
P = applied pressure

Depth (z/b)	Vertical Stress (P) y/b = 0	y/b = 0.50	y/b = 1.0
0	1.0000	1.000	0.5
0.1	0.99958	0.99832	0.4997
0.2	0.99676	0.98815	0.49979
0.3	0.98967	0.96679	0.49930
0.4	0.97729	0.93679	0.49838
0.5	0.95948	0.90223	0.49692

TABLE 4

BRIEF DESCRIPTION OF THE FUNCTION OF
RADIO LINK TRANSMISSION COMPONENTS

INSTRUMENT	COMPONENTS	DESCRIPTION OF FUNCTION
Probe	Sensor	converts the measured pressure into electrical signals
	Sensor Interface	provides temperature compenstated electrical signals, voltage or current proportional to the pressure exerted upon the sensor
	A/D Converter	converts the analog signals to digital information
	Processor	takes the digital output from the A/D Converter and processes, stores, and formats it for transmission
	Modulator	modulates the digital signals onto the carrier RF signal
	Transmitter	contains oscillator and low power RF amplifier circuits with antenna matching network
	Antenna Switch	switches the antenna from receiver input to transmitter output as directed for the model processor
	Antenna	consists of isolated cable and could be in the form of dipole (two wires) or 'ground plane' (single wire working against the body of probe)
	Receiver	uses low power consumption circuits (CMOS) and will be on constantly (or preprogrammed intervals)
	Mode Processor	(could be part of processor) will be turned on when activated by remote instrument. This processor will activate all necessary circuits in proper order and control sequence and operation of whole probe. When the measurement cycle is completed, it will shut-off circuits except the receiver.
	Battery	should be of long life, high capacity/volume type

NOTE: Refer to Figure 6 for block diagrams of the components

...cont'd

TABLE 4 (cont'd)

INSTRUMENT	COMPONENTS	DESCRIPTION OF FUNCTION
Transmission Instrument	Transmitter	contains oscillator and power amplifier and is activated by the processor
	Antenna Switch	switches the antenna between transmitter and receiver
	Receiver	receives signals from the antenna and demodulates them. They can be recorded by the recorder and/or processed by the instrument.
	Recorder	can be small unit using microcassettes
	Decoder	decodes signals received by the receiver and shapes the pulses. The output will be in digital form suitable for further processing
	Storage	allows burst of data to be stored or received from the probe
	Processor	processes the information received and format it for the display
	Display	LCD type, low power consumption. It will display measured data as transmitted by the probe. Cassettes with recorded data can be also processed in the lab using compatible laboratory equipment.

NOTE: Refer to Figure 6 for block diagrams of the components

TABLE 5

COST ESIMATE FOR RADIO LINK TRANSMISSION SYSTEM

Development (to produce prototype working circuit)

a. Probe

Parts	$ 500.00	
Labour	12000.00	
Contingency	4000.00	
		$16,500.00

b. Transmission Instrument

Parts	$ 600.00	
Labour	10000.00	
Contingency	2500.00	
		$13,100.00
TOTAL		$29,600.00

Production - Unit Cost

a. Probe

Parts	$ 750.00	
Labour	2110.00	
Contingency	527.00	
		$ 3,387.00

b. Transmission Instrument

Parts	$ 1200.00	
Labour	4220.00	
Contingency	1055.00	
		$ 6,475.00
TOTAL		$ 9,862.00

TABLE 6

SUMMARY OF COST ESTIMATES
FOR LOAD CELLS AND STRESS MONITORING PROGRAM

Type of Load Cell Stress Monitoring	ESTIMATED COST ($)				
	Hardware	Installation	Output Data Transmission a. Cable Link b. Radio Link	Calibration	Estimated Delivery Time
1. Oil-filled Load Cell	4,750	10,000	a. $9/m (cable) 4500 (readout) b. 40,000	3,000	8 weeks
2. Displacement Load Cell	6,500	10,000	a. $12/m (cable) 4500 (readout) b. 40,000	3,000	12-16 weeks
3. Capacitance Load Cell	3,000 (plus initial development cost of $25,000)	10,000	a. $12/m (cable) 4500 (readout) b. 40,000	3,000	subject to development
4. Stress Change	8,000 (including drilling)	*4,600	3,000 (readout)	stress meter is factory calibrated	2-4 weeks for stress meters

NOTES: (1) See Section 4.6 in text for description of items included in each cost component.

(2) Installation cost was based on 180 man-hours

* Assuming rental installation unit available.

CONFIGURATION OF POWERED SUPPORT SYSTEM AT LONGWALL COAL FACE

FIGURE 1

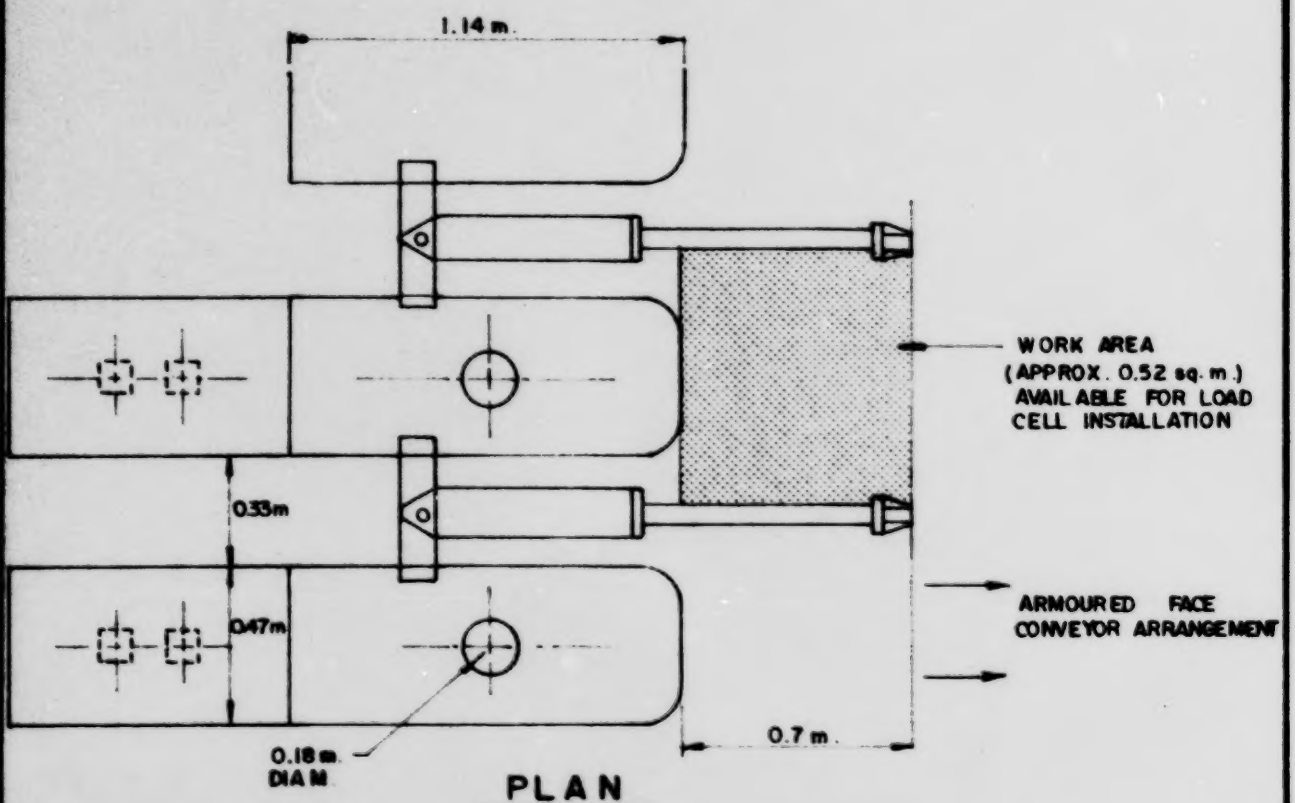

PLAN

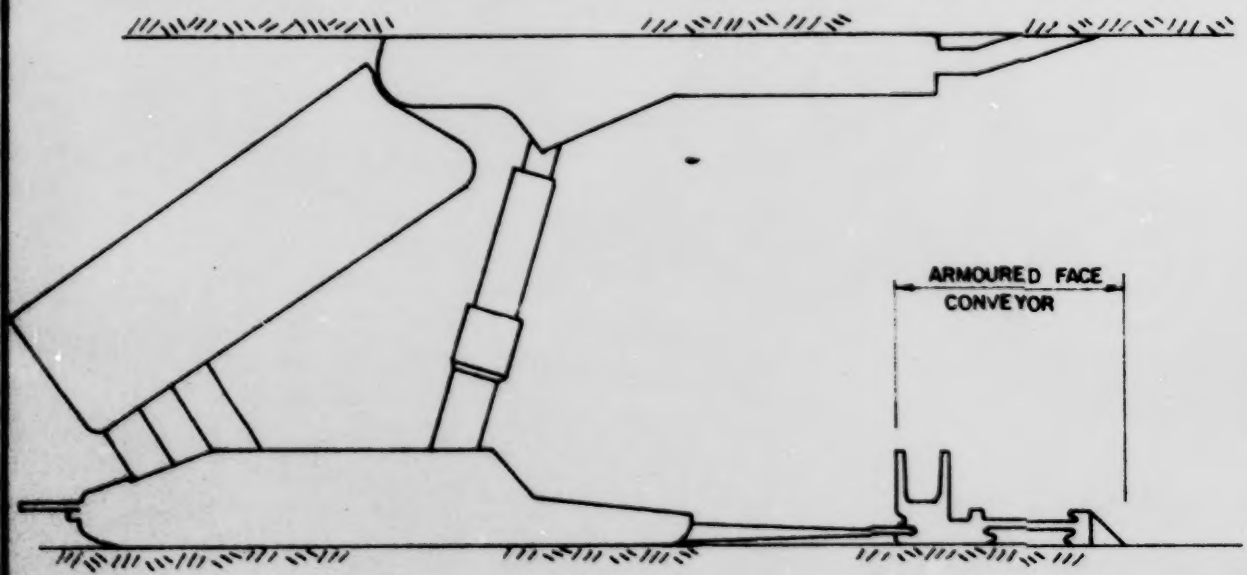

WEB - BACK MODE

NOT DRAWN TO SCALE

Date DEC. 7, 1984
Project 841-1251

Golder Associates

Drawn G.P.
Chkd.

CONCEPTUAL DESIGN OF OIL FILLED LOAD CELL

FIGURE 2

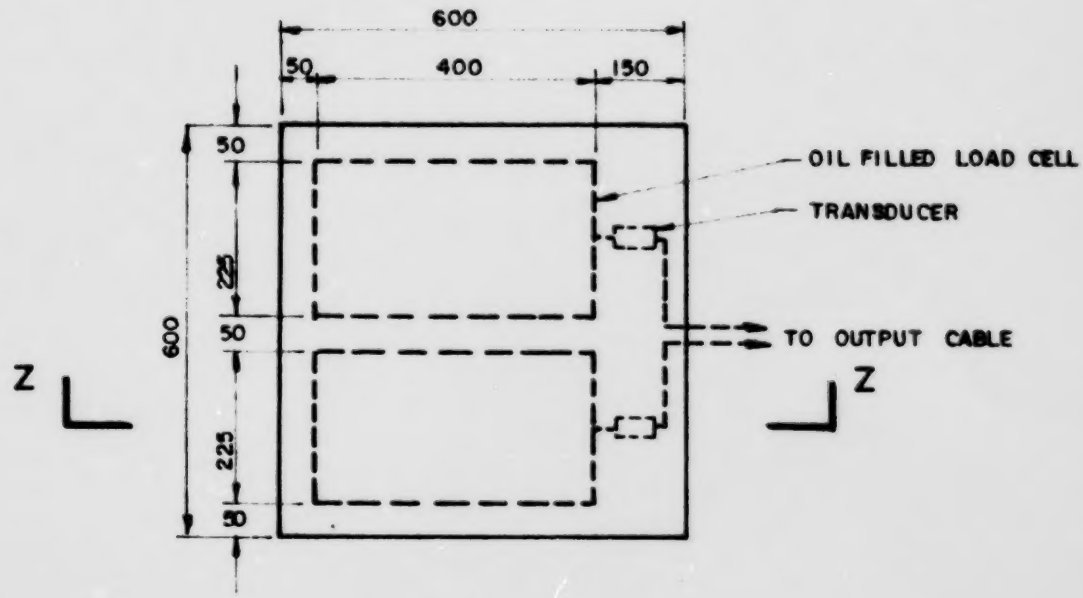

PLAN

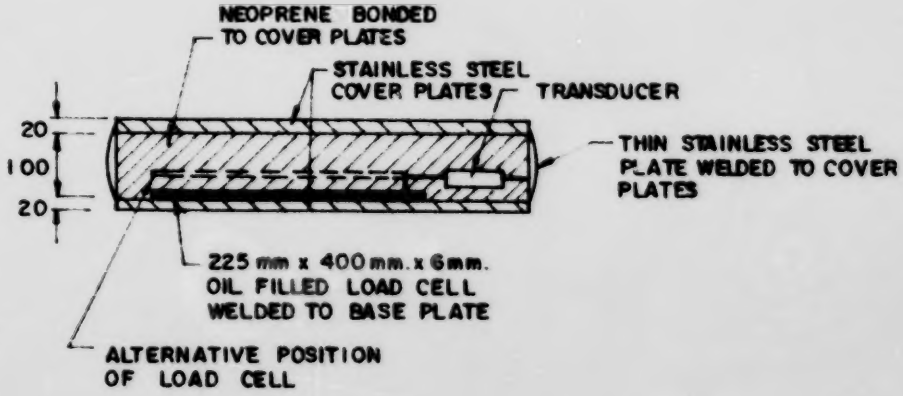
NEOPRENE BONDED TO COVER PLATES
STAINLESS STEEL COVER PLATES
TRANSDUCER
20
100
20
THIN STAINLESS STEEL PLATE WELDED TO COVER PLATES
225 mm x 400 mm. x 6mm. OIL FILLED LOAD CELL WELDED TO BASE PLATE
ALTERNATIVE POSITION OF LOAD CELL

SECTION Z-Z

NOTE

ALL DIMENSIONS ARE IN MILLIMETRES.

SCALE 1:10

Date DEC. 7, 1984
Project 841-1691

Golder Associates

Drawn D.M
Chkd.

CONCEPTUAL DESIGN OF DISPLACEMENT LOAD CELL

FIGURE 3

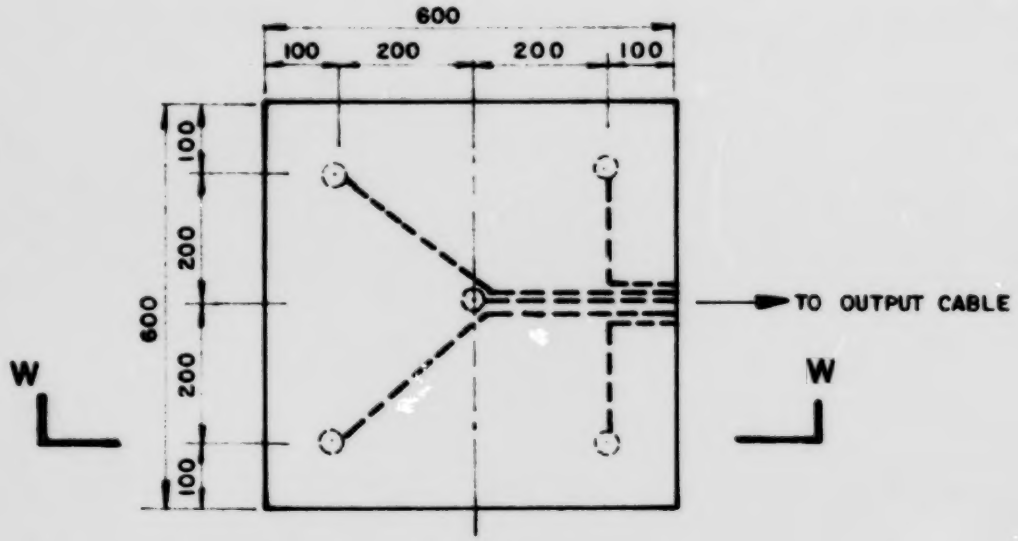

PLAN

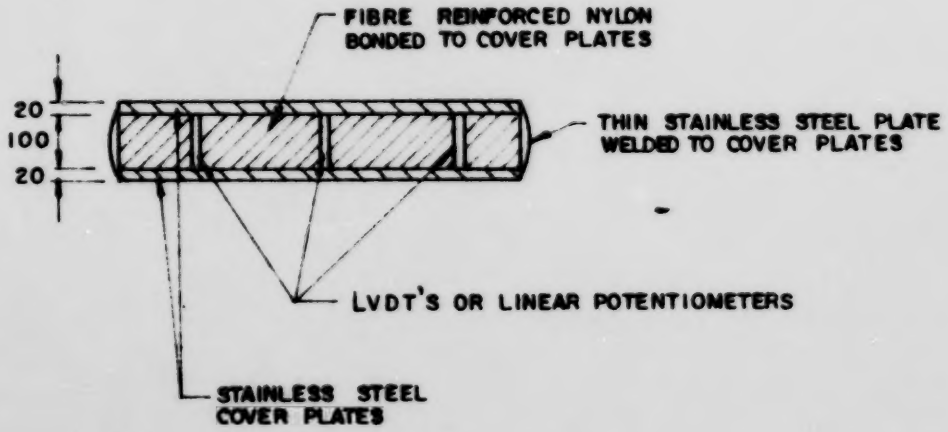

SECTION W-W

NOTE

ALL DIMENSIONS ARE IN MILLIMETRES.

SCALE 1:10

Date DEC. 7, 1984

Project 841-1251

Golder Associates

Drawn D. M.

Chkd

CONCEPTUAL DESIGN OF CAPACITANCE LOAD CELL

FIGURE 4

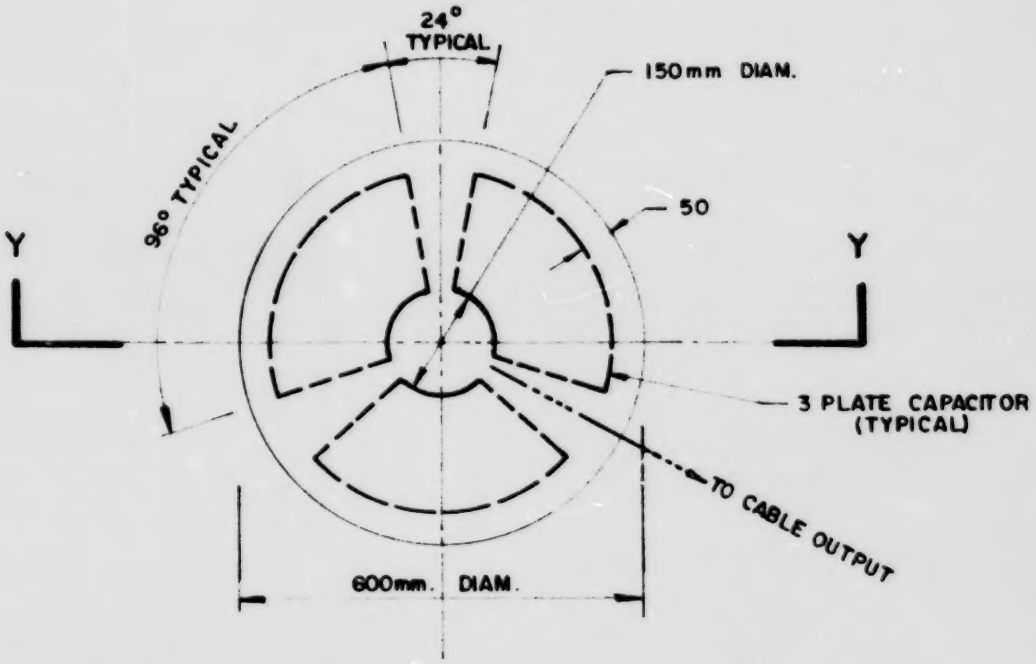

PLAN

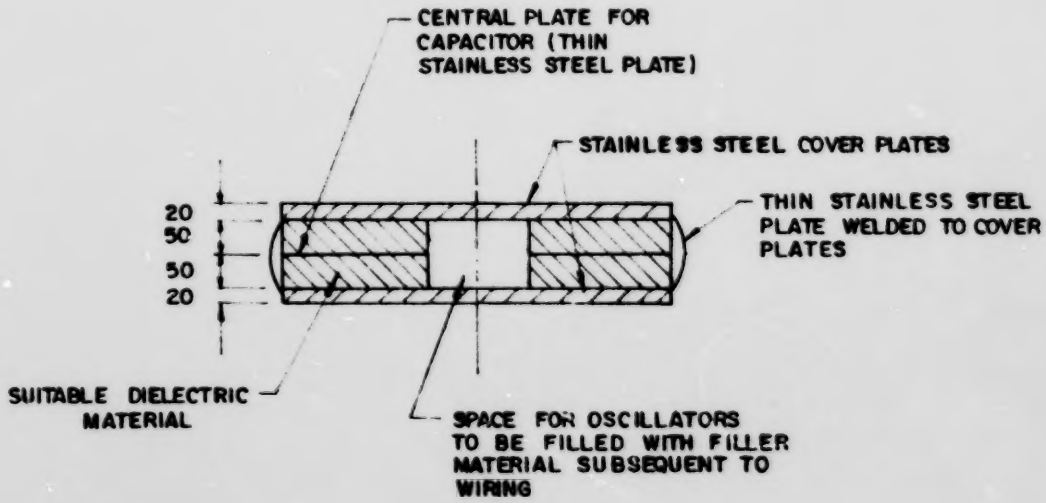
CENTRAL PLATE FOR CAPACITOR (THIN STAINLESS STEEL PLATE)
STAINLESS STEEL COVER PLATES
THIN STAINLESS STEEL PLATE WELDED TO COVER PLATES
20
50
50
20
SUITABLE DIELECTRIC MATERIAL
SPACE FOR OSCILLATORS TO BE FILLED WITH FILLER MATERIAL SUBSEQUENT TO WIRING

SECTION Y-Y

NOTE

ALL DIMENSIONS ARE IN MILLIMETRES.

SCALE 1 : 10

Date DEC. 7, 1984

Project 841-1251

Golder Associates

Drawn D.M.

Chkd

LAYOUT OF BOREHOLE FOR STRESS MONITORING

FIGURE 5

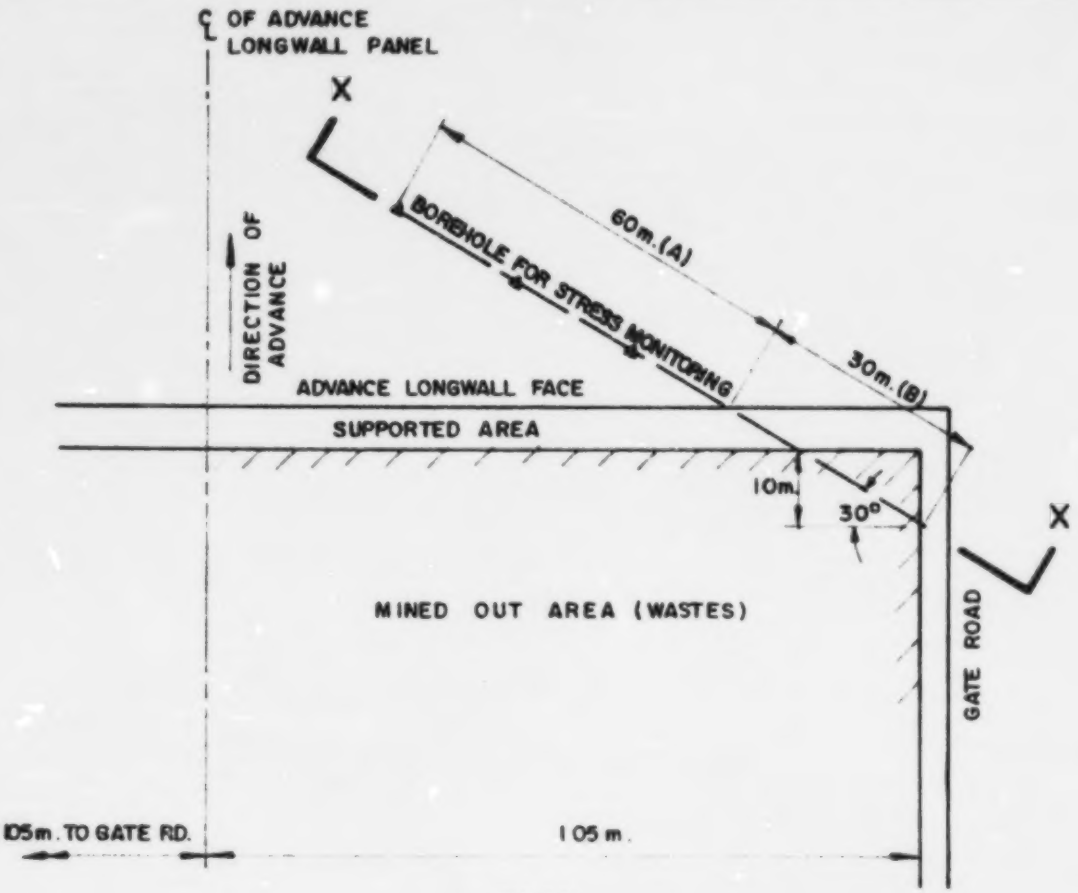

PLAN

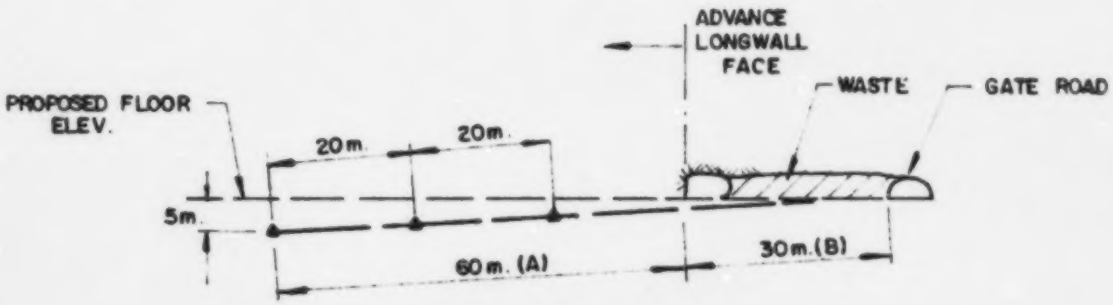

SECTION X-X

LEGEND

▲ - PROPOSED VW STRESS METER POSITION

(A) - SECTION DRILLED TO 'E' SIZE (38mm. DIAM.)

(B) - SECTION DRILLED TO 'A' SIZE (48mm. DIAM.) LINED WITH EW CASING

SCALE 1:1000

Date DEC. 7, 1984

Project 841-1251

Golder Associates

Drawn D.M.

Chkd

BLOCK DIAGRAMS OF PROBE AND TRANSMISSION INSTRUMENT FOR RADIO LINK TRANSMISSION

FIGURE 6

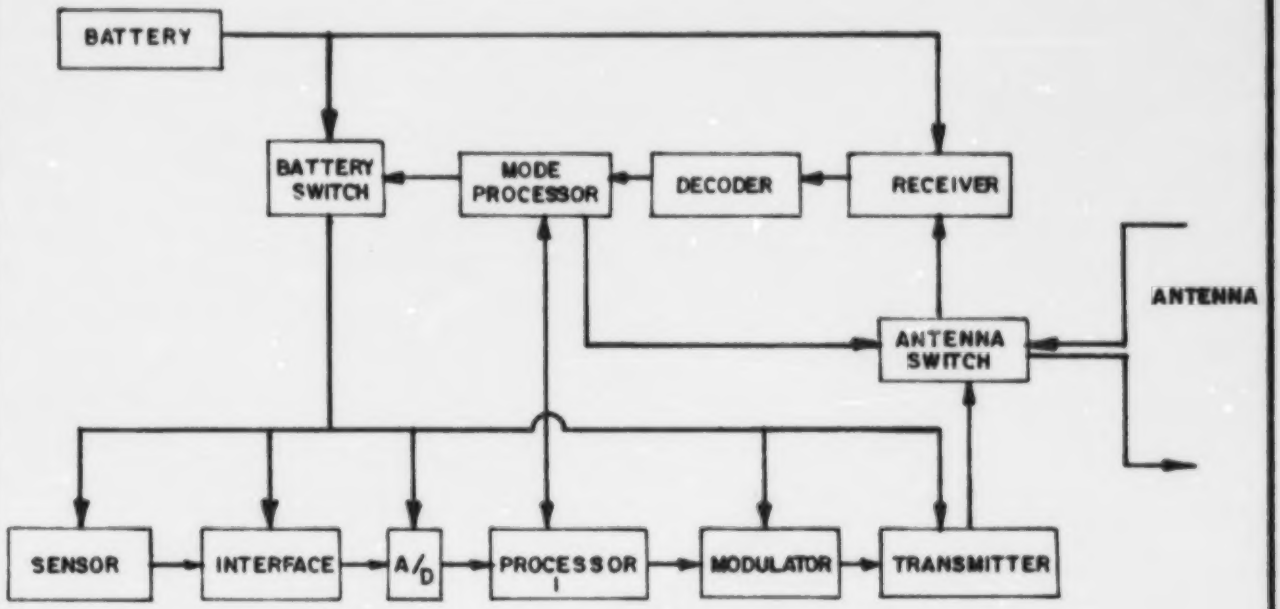

A) BLOCK DIAGRAM - PROBE

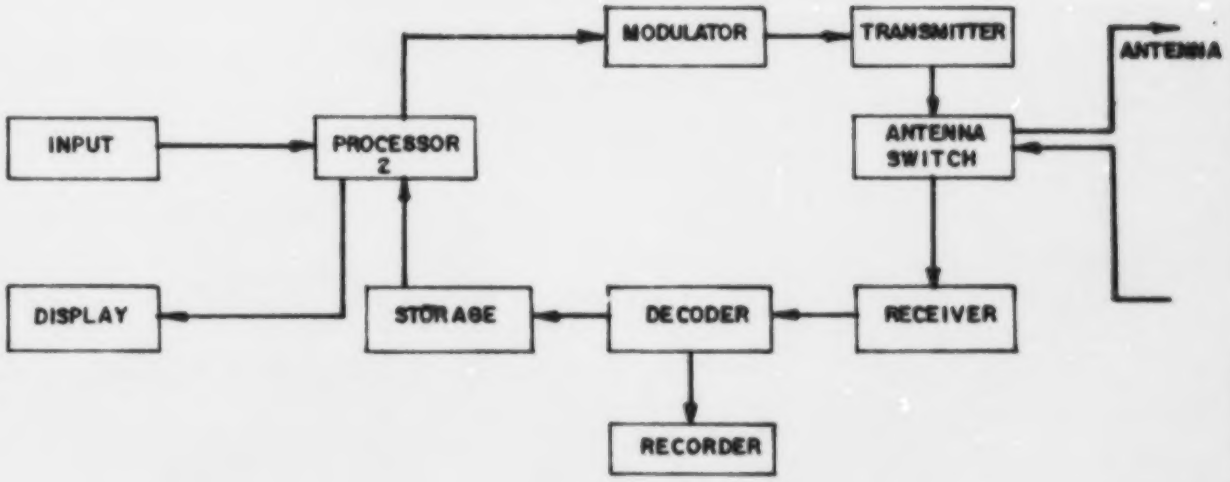

B) BLOCK DIAGRAM - TRANSMISSION INSTRUMENT

Date DEC. 5, 1984
Project 841-1251

Golder Associates

Drawn D.M.
Chkd

FORM 3 A.-3

TYPICAL INSTALLATION OF LOAD CELL

FIGURE 7

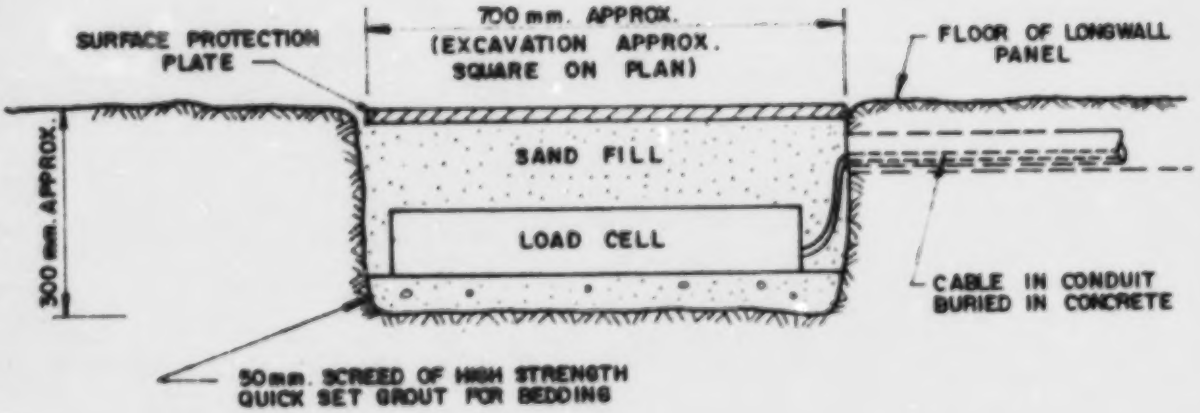

SCALE 1:10

Date DEC. 7, 1984
Project 841-321

Golder Associates

Drawn D. M.
Chkd.

Golder Associates
CONSULTING GEOTECHNICAL AND MINING ENGINEERS

REPORT TO
CANMET

DESIGN, DEVELOPMENT AND MANUFACTURING OF A RUGGED LOAD CELL TO MONITOR AND RECORD LOAD IN LONGWALL WASTES PHASE 2

SYDNEY NOVA SCOTIA

DSS CONTRACT NO. 0SQ84-00161

Distribution:

15 copies - Cape Breton Coal Research Laboratory
Sydney, Nova Scotia

2 copies - Golder Associates
Mississauga, Ontario

OCT 23 1985
MICROMEDIA

63 pp

March 1985

841-1251

ABSTRACT

In connection with the design, development and manufacturing of a rugged load cell for measuring loads in longwall wastes, a calibration program for the Irad Gage vibrating wire stressmeters was undertaken in Phase 2 of the study.

Five stressmeters equipped with SR (soft rock) platens and manual installing tools were acquired. The calibration was carried out using a sandstone block in which the stressmeter was installed. The block was subjected to known applied uniaxial stresses, and axial strains in the block were measured.

The results indicated that the vibrating wire stressmeter would provide reasonable assessment of uniaxial stress changes provided that good and even contact is developed at the stressmeter - rock interface. Mal-alignment of the gauge by ±5° may lead to an under-estimate of the stress change by 2 to 10% whereas a deviation of ±10° may increase the error to about 15%.

Due to seating adjustment occurring at the stressmeter bore-hole interface, there would be a finite but relatively short term creep in the stressmeter reading during the initial period of installation.

RESUMÉ

En rapport avec la conception, le développement et la fabrication d'une capsule manométrique robuste pour la mesure des charges causées par l'affaissement des lits stériles derrière une longue taille, un programme visant à la calibration d'indicateurs de contraintes (Vibrating Wire Stressmeters) fabriqués par Irad Gage fut entrepris dans cette seconde phase de l'étude.

Cing indicateurs de contraintes, munis de plateaux SR (pour roches molles) et l'équipement nécessaire pour l'installation manuelle furent acquis. Les indicateurs de contraintes furent calibrés en utilisant un bloc de grès pourvu d'un orifice permettant l'installation de ces-derniers. Le bloc fut soumis à des contraintes uniaxiales d'intensités connues. La déformation du bloc, dans la direction de la contrainte, fut mesurée

Les résultats ont montré que les indicateurs de contraintes permetteraient une évaluation raisonnable des variations dans la contrainte uniaxiale à condition que le contact à l'interface entre la roche et l'indicateur soit uniforme et bon. De plus, un mauvais alignement de l'indicateur de ±5° peut entraîner une sous-évaluation des variations de la contrainte entre 2 et 10%; alors qu'une déviation de ±10° peut augmenter l'erreur jusqu'à environ 15%.

Enfin, à cause du ré-ajustement qui se produit à l'interface entre l'indicateur et le périmetre du trou, les lectures initiales montreront des signes de fluage qui est, toutefois, de courte durée.

TABLE OF CONTENTS

	Page No.
ABSTRACT	i
1.0 INTRODUCTION	1
2.0 BACKGROUND DATA	2
2.1 Objective of the Study	2
2.2 Summary of Phase 1 Study	2
3.0 CALIBRATION OF VIBRATING WIRE STRESSMETER	4
3.1 Brief Description of the Irad Gage Vibrating Wire Stressmeter	4
3.2 Calibration Program	5
3.3 Calibration of Stressmeter under known Uniaxial Loading Conditions	6
3.3.1 Test Procedure	6
3.3.2 Test Results	7
3.4 Calibration of the Variation in the Response of the Stressmeter with Angular Rotation from Direction of Applied Load	11
3.5 Evaluation of Long Term Creep of the Stressmeter	11
4.0 COMPUTATION OF NEW PRINCIPAL STRESSES FROM STRESS CHANGES IN A THREE-DIMENSIONAL STRESS FIELD	13
5.0 DATA ON DIEELECTRIC MATERIAL FOR CAPACITANCE LOAD CELL	14
6.0 CONCLUSIONS	15
APPENDIX A: Computation of New Principal Stresses From Measured Stress Changes	
APPENDIX B: Dielectric Materials	

LIST OF TABLES

1. Calibration Test Program

2. Physical Properties of Pier Cap Sandstone

3. Summary of Test Conditions for Vibrating Wire Stressmeters

4. Calibration of Stressmeter Under Uniaxial Loading Conditions, Data Summary and Reduction

5. Typical Strain Measurements During Calibration of Stressmeter Under Uniaxial Loading Conditions

6. Comparison of Actual and Thoretical Slopes in the Stress vs $\frac{1}{T^2}$ Relationships

7. Effects of Angular Rotation on Stress Change Measurements

8. Evaluation of Long Term Creep.

LIST OF FIGURES

1. Stressmeter Uniaxial Sensitivity (SR), Test T2-01-0A, VBS2 (3-29)

2. Stressmeter Uniaxial Sensitivity (SR), Test T2-10-0B, VBS2 (3-29)

3. Stressmeter Uniaxial Sensitivity (SR), Test G1-01-0A, VBS2 (217)

4. Stressmeter Uniaxial Sensitivity (SR), Test G1-10-0B, VBS2 (217)

5. Stressmeter Uniaxial Sensitivity (SR), Test G2-01-0, VBS2 (10.7)

6. Stressmeter Uniaxial Sensitivity (SR), Test G2-02-0, VBS2 (10.6)

7. Stressmeter Uniaxial Sensitivity (SR), Test G2-03-0, VBS2 (10.51)

8. Applied Stress vs $\frac{1}{T^2}$, Tests T2-01-0A and T2-10-0B

9. Applied Stress vs $\frac{1}{T^2}$, Tests G1-01-0A and G1-10-0B

10. Applied Stress vs $\frac{1}{T^2}$, Tests G2-01-0 and G2-02-0

11. Applied Stress vs $\frac{1}{T^2}$, Test G2-03-0

12. Effect of Stressmeter Installation Angle on Measured Stress Changes

13. Coordinate Systems for Evaluation of Insitu Stresses

LIST OF PLATES

1. Readout unit, stressmeter and instrumented sandstone block

2. Installation of the stressmeter in the preloaded sandstone block

1. INTRODUCTION

Golder Associates was awarded a contract (DSS Contract No. 0SQ84-00161) by the Department of Supply and Services through the auspices of CANMET to undertake a program of design, development and manufacturing of a rugged load cell to be used to measure loads in longwall wastes.

The project is divided into two phases. Phase 1 was completed in December 1984 and entailed the conceptual design of the load cells with cost estimates for the proposed options. One of the options is to measure stress changes in the rock mass by means of sensing instruments installed below the floor of the longwall panel. This was considered, by the Scientific Authority, to be the most appropriate for the project at present. Accordingly, Phase 2 comprises the acquisition of five (5) vibrating wire stress-meters complete with installation tools, and laboratory calibration of these instruments in preparation for their implementation in the Sydney Coalfield.

2. BACKGROUND DATA

2.1 Objective of the Study

The success of longwall coal mining depends upon the progressive collapse of the strata above and behind the working face as that face advances through unmined ground. The strata collapse into the mined-out area (gob) which fills with debris and gradually compacts as the mined-out area progressively advances. The characteristics of this compaction within the gob indirectly control the nature of subsidence development above the worked out areas and in turn, has an important bearing upon the mineability of overlying coal seams and the leakage of groundwater into the workings when the mines are located under surface bodies of water as is frequently the case in the Sydney Coalfield.

For these reasons, the load transferring capability of the collapsed material (wastes) in the gob is of significance in understanding and controlling the development of longwall mining techniques. Very little is known about this phenomenon because of difficulty in obtaining accurate measurements from an area which is hazardous to human entry. The objective of the present investigation is to develop techniques and equipment which will permit the accurate measurement of load distributions below the gob, both in the centre of the area which can be expected to be unaffected by the limits of the excavation, and closer to the roadways where the load sharing effect of the unmined pillars may be expected to play a significant part in the load transfer capabilities of the waste material.

2.2 Summary of Phase 1 Study

In the Phase 1 report, a range of design options have been considered for monitoring the loading from the wastes in a longwall panel. Because of the high load capacity required

for the load cell, existing commercially available load cells cannot be directly applied to meet the design requirements. The findings of Phase 1 are summarized below.

- Four possible load measuring designs were examined, they included: oil filled load cell, displacement load cells, capacitance load cell and measurement of stress changes in the rock mass by means of borehole stressmeters. The technology for oil filled load cell has been developed and no major technical difficulties are anticipated in manufacturing a prototype. The technologies for the manufacturing of the components of the displacement and capacitance load cells have also been developed. However, prior to manufacturing a prototype further investigation into the availability of a suitable filler or dielectric material (which exhibits very small long term creep) will be required.

- The monitoring of stress changes is technically feasible and should provide a reasonable assessment of the average loading from the wastes.

- The use of radio link for transmission of output signals from the instrument is very attractive for the present application, but the development cost is substantially higher than the cable link option.

- It was recommended that the oil filled load cell be manufactured and the field trial be augmented by the stress monitoring scheme.

3. CALIBRATION OF VIBRATING WIRE STRESSMETER

This section describes the type of stressmeters acquired, and the laboratory equipment and procedure used for the calibration program.

3.1 Brief Description of the Irad Gage Vibrating Wire Stressmeter

The stressmeters acquired for Phase 2 of the study were manufactured by Irad Gage, Inc. of Lebanon, New Hampshire and were the type designated as VBS2 with soft rock (SR) platen One set of manual installation tool (sufficient for 10 m installation) was also supplied with the stressmeters. The MB6 readout unit was used for reading the frequency of the vibrating wire.

The vibrating wire stressmeter (Irad Gage Instruction manual) consists of a hollow steel cylinder which, in use, is pre-loaded diametrically across the sides of an EX (38 mm dia.) borehole by means of a sliding wedge and platen assembly. Stress changes in the surrounding rock cause small changes in the diameter of the cylinder which are measured as changes in the natural frequency of vibration of a highly tensioned steel wire stretched diametrically across the cylinder walls in the preload direction. By calibration, changes in the wire period (time for one cycle of vibration) have been related to the magnitude of stress changes for a range of rock type. In higher modulus rock, stress changes of up to 69 MPa (10,000 psi) can be monitored whereas in softer material, the range is about 42 MPa (6,000 psi).

The stressmeters tested were provided with the SR (soft rock) platens assembly as described. These platens are 31.8 mm (1.25 in.) wide with a radius of curvature of

19.8 mm (0.75 in.). The serial numbers of the five stressmeters are as follows:

- VBS2 (217)
- VBS2 (3-29)
- VBS2 (10.6)
- VBS2 (10.51)
- VBS2 (10.7)

3.2 Calibration Program

The laboratory calibration program for the stressmeter included the following aspects:

(a) to evaluate the performance of the stressmeter under known uniaxial loading conditions;

(b) to examine the variation in the response of the stressmeter with respect to the angular deviations from the direction of applied loading;

(c) to assess the long term creep of the stressmeter; and

(d) to provide guidelines for the installation of the instruments on the basis of the calibration.

Aspects (a) and (b) were undertaken by installing the stressmeters in a sandstone block which was subjected to known applied stresses. The features of the tests involved in these aspects are presented in Table 1.

The sandstone material used for the calibration tests is a light-grey, homogeneous, medium grained, Pier Cap Sandstone obtained from a local supplier. Table 2 summarizes the physical properties of the Pier Cap Sandstone. A 75.4 mm x 197.1 mm x 266.7 mm (2.97 in. x 7.76 in. x 10.5 in.) block was cut and prepared for the test. Both ends of the block

were ground for smoothness and parallelism. An EX (38 mm dia.) hole was drilled at the centre of the block for the insertion of the stressmeters (see Plate 1).

The calibration tests were performed using both the 1.2 MN Louis Small C-CP250 concrete tester of the University of Toronto and the Forney compression rig model QC50 of Golder Associates. In order to assess the uniformity of loading across the block, electrical resistance wire strain gauges were used to monitor the axial strain in the block during the loading process. Eight gauges were installed (four on each side of the block) at approximately 25.4 mm (1.0 in.) from the top edge of the block and 40 mm apart (see Plate 1).

3.3 Calibration of Stressmeters under Known Uniaxial Loading Conditions

3.3.1 Test Procedure

In this series of test, the sandstone block was initially subjected to an axial seating load of at least 22.3 kN (5,000 lbf) which is equivalent to 1.5 MPa (217 psi) of axial stress. Higher seating load, of up to 71.2 kN (16,000 lbf), corresponding to 4.8 MPa (695 psi) of axial stress, was also used in a number of tests (see Table 3). The preload was applied to take out the initial slack in the system and to prevent induced tensile fracturing around the hole which could result from the pressure from insertion in an otherwise unstressed block. (During the preliminary stage of the calibration program, a block was split when the stressmeter was installed with no preloading).

The stressmeter was then inserted into the EX size hole and preloaded (preset) by means of the manual installation and setting tool, with the vibrating wire aligned in the direction of the applied axial stress (see Plate 2). Readings were taken using the MB6 readout unit before (initial

reading) and after (preset reading) the instrument was installed. Table 3 summarizes the testing conditions including the instrument serial numbers, the test reference numbers, the preloading on the sandstone, and the initial and preset readings of the stressmeters.

The strain gauge readings were set to zero prior to preloading the block. Readings were taken after application of the preload and installation of the stressmeter.

Axial loading on the block was then increased in increments varying from 40.1 to 75.7 kN (9000 to 17000 lbf) to a maximum of 445 kN (100,000 lbf). The maximum load applied varied with individual tests. Unloading was undertaken in larger load intervals due to the difficulties in controlling the load decrements in the testing machines. Readings of the stressmeters and strain gauges were recorded at each stage of loading and unloading.

3.3.2 Test Results

The measured data obtained from the calibration tests in this series are summarized in Table 4. Typical strain gauge readings during loading and unloading of the block are shown in Table 5.

On the basis of the recorded data, the performance characteristic of the stressmeters under various testing conditions was evaluated by reducing the data in the format as presented in Table 4 (data reduction).

Calculated Stress Change

The calculated stress change was derived on the basis of the following expression given by Irad Gage Inc. (installation manual).

$$\sigma_r = \frac{\left[\frac{422400}{T_o}\right]^2 \left[1 - \left(\frac{T_o}{T}\right)^2\right]}{11.4 - 0.66 \times 10^{-6} E_r} \quad (1)$$

where σ_r = change in uniaxial rock stress (psi)

T_o = previous meter reading

T = current meter reading

E_r = modulus of elasticity of rock (psi)=2.11 x 10^6 psi (14.5 GPa) (determined from stress-strain relationship of sandstone block)

The incremental stress change is also presented to facilitate subsequent calculation of the sensitivity factors.

Equation 1 can be rewritten in the following form.

$$\sigma_r = \frac{422400^2}{11.4-0.66\ E_r x 10^{-6}} \left[\frac{1}{T_o^2} - \frac{1}{T^2}\right] \quad (2)$$

For E_r = 2.11 x 10^6 psi

$$\sigma_r = 17.82 \times 10^9 \left[\frac{1}{T_o^2} - \frac{1}{T^2}\right] \quad (3)$$

$$= \frac{17.82 \times 10^9}{T_o^2} - \frac{17.82 \times 10^9}{T^2} \quad (4)$$

Taking T_o as the intial preset reading, the plot of σr and $\frac{1}{T^2}$ would be linear. For the purpose of subsequent comparison, the values of $\frac{1}{T^2}$ were also calculated and presented in the data reduction Table 4.

Gauge Uniaxial Sensitivity

The gauge uniaxial sensitivity is defined as the change in uniaxial stress (psi) per unit change in meter readings. The calculated and actual gauge sensitivies are derived as follows:

$$\text{Calculated gauge senstivity} = \frac{\text{Calculated Incremental stress change}}{\Delta T}$$

$$\text{Actual gauge sensitivity} = \frac{\text{Applied Incremental stress change}}{\Delta T}$$

where ΔT = incremental stressmeter reading

These two factors are presented in Table 4 for comparison purposes.

Comparison of Calculated and Actual Stress Changes

The interpretation of stress changes from the changes in the stressmeter reading are given in Irad Gage manual in two graphical forms. The first one is the plot of the gauge sensitivity with meter reading and the second, the plot of stress changes with meter readings. The results obtained from the calibration tests are, however, presented in a slightly modified form. Basically, two series of plots are presented. The first series comprises plots of gauge sensitivity vs meter reading (Figures 1 to 7), similar to the format in the manual. The second series consists of plots of stress changes vs the inverse square of the meter reading ($\frac{1}{T^2}$), Figure 8 to 11.

For comparison purposes, both the calculated and actual stress changes are plotted for each stressmeter for the loading and unloading conditions. The second series of plots provide a better basis for comparison because the slopes of straight lines can be readily compared.

The observations made from the plots are summarized below:

(a) On the basis of the incremental strain readings, the applied loading on the block was reasonably uniform within the central half of the block.

(b) A comparison of the slopes of the applied stress vs $\frac{1}{T^2}$ plots is presented in Table 6. In general, the agreement between the actual and calculated stress changes is better for installation with higher preset. The best fit occurs in test G2-02-0 with a preset of 116 units. While there is no definitive correlations of preset with the observed discrepancies, it is obvious that a high preset would ensure better contact between the platen and the surface of the hole. The unloading data are consistent with the data gathered during loading.

(c) The results of the gauge sensitivity vs meter readings plots present similar trend to the $\frac{1}{T^2}$ plots. The best agreement occurred in test G2-02-0 and for a majority of the range in test G2-01-0. In the rest of the tests, the actual sensitivity is generally higher but the discrepancy tends to decrease with increase in meter loading (that is, increase in load).

In summary, it may be concluded that the stressmeter would give reasonable assessment of the unidirectional stress changes in the rock provided that there is good gauge and borehole contact. Otherwise, the stress changes in the rock would be under-estimated. The effect of angular deviation of stressmeter from the desired orientation on the stress changes are discussed in the next section.

In shallow hole installation of up to about 10 m depth, manual installation tool can be used but in deep hole installation hydraulic installation tools are required to ensure good gauge-rock contact.

3.4 Calibration of the Variation in the Response of the Stressmeter with Angular Rotation from the Direction of Applied Load

These tests were carried out to determine the effects of variation in the angle between the vibrating wire (or vertical axis of the stressmeter) and the direction of applied stress. Two series of tests were performed using stressmeter VBS2 (217) and VBS2 (3-29).

For each series, the Sandstone block was preloaded to 71.2 kN (16,000 lbf) when the stressmeter was installed. The load was then increased in increments to 373.8 kN (84,000 lbf). The tests were undertaken with the installed orientations of the stressmeter ranging from α=0° to 45° (see Table 7). For assessing the influence of the variation in angular rotation of the stressmeter, the stressmeter readings between the loading interval of 298.2 kN (67,000 lbf) and 373.8 kN (84,000 lbf) were used as the basis for evaluating the calculated stress changes using equation 1 in Section 3.3.2. The calculated stress changes at different α were expressed as a percentage of that at α=0° and summarized in Table 7.

It may be noted that if the stressmeter is installed at ±10° (α=10°) with respect to the desired orientation, the error in the calculated stress changes would be within 15 percent. As the angular deviation increases, the error increases significantly (see Figure 12).

3.5 Evaluation of Long Term Creep of the Stressmeter

In this test, a stressmeter was positioned within an unloaded sandstone overcore obtained during the stress measurement program at No. 26 Colliery. The stressmeter was installed with a preset of 140 units. The change in readings with time was monitored and presented in Table 8. The readings

decreased slowly and stabilized after a reduction of 21 units in about 3 days. On the basis of the creep test results, it should be noted that some relaxation of the preset reading would occur during the initial stage of monitoring. Hence, in planning the field program, some allowance should be made for the instruments to attain equilibrium condition.

4. COMPUTATION OF NEW PRINCIPAL STRESSES FROM STRESS CHANGES IN A THREE-DIMENSIONAL STRESS FIELD

The stressmeter provides measurement of the uniaxial stress changes in the direction of the vibrating wire. The computation procedure has been given in Section 3. With the installation of three stressmeters at known orientations, the secondary principal stress changes on the plan perpendicular to the axis of the borehole can be evaluated. If a local co-ordinate system (h_1, h_2 and h_3) as illustrated in Figure 13 is defined for the borehole, the components of stress changes with respect to the local co-ordinates system can be evaluated. These stress components can then be superimposed on the initial stress system (with respect to the same co-ordinate system) to obtain the new absolute stresses.

If similar measurements and computations are undertaken in a second, non-orthogonal borehole, the new absolute stresses with respect to the local co-ordinates of the second boreholes can also be evaluated.

The new absolute stresses can further be resolved into components with reference to a common global co-ordinate system (x, y, z) which may conform with the mine co-ordinate system. The new stress components are σ_x, σ_y, σ_z, T_{xy}, T_{yz}, T_{zx} based on which the new principal stresses can be evaluated.

Hence, if the initial insitu stresses are known, the new three-dimensional state of stress can theoretically be determined by installing a minimum of six stressmeters, three in each non-orthogonal boreholes.

An outline of the procedures for the computation of the new principal stresses is presented in Appendix A.

5. DATA ON DIELECTRIC MATERIAL FOR CAPACITANCE LOAD CELL

Further research toward the determination of an appropriate dielectric material for use in a capacitance load cell was also pursued in the second phase of the project. Two major plastic manufacturers were contacted, Ciba-Geigy Canada Ltd. and Dupont Canada Inc.

Both manufacturers were briefed on the usage that would be made of the material and the general requirements for the material properties:

- high strength
- high impact strength
- elastic behaviour
- low creep
- good dielectric properties

Each of the manufacturers provided technical specifications on product(s) they believe would meet the above requirements. The recommended products include:

- Ciba-Geigy: Araldite 507
- Ciba-Geigy: Araldite 502
- Dupont: Rynite

Appendix B lists the relevant data on the material properties.

6. CONCLUSIONS

In connection with a program of design, development and manufacturing of a rugged load cell to be used to measure loads in longwall wastes, a program of calibration of vibrating wire stressmeters have been undertaken in Phase 2 of the study. The conclusions derived from the calibration program summarized below:

(a) The results of the calibration tests indicated that the vibrating wire stressmeter would provide reasonable assessment of uniaxial stress changes provided that good and even contact is developed at the stressmeter-rock interface. Based on the stress change vs $\frac{1}{T^2}$ plots for all the calibration tests, the variation between the measured and calculated stress changes ranges from approximately -6% to 27% (Table 6). While there is no distinct correlation between the preset reading and the discrepancy between the calculated and measured stress changes, the accuracy appears to be generally better with higher preset. The agreement between the measured and calculated gauge sensitivities (stress change per unit change in meter reading) generally improves with increase in meter reading (ie. increase in applied stress) due probably to better and more even contact between the gauge and the rock.

(b) Mal-alignment of the gauge by ±5° may lead to an underestimate of the stress change by 2 to 10% whereas a deviation of ±10° may increase the error to about 15%. Further increase in error would occur with larger deviations. It is important therefore that the orientation of the gauge be set as accurately as possible during installation. Depsite the use of oriented rods for placement of the gauge, the use of a mercury switch attached to the first setting rod would help to control the alignment of the gauge prior to setting it in place.

(c) As good contact between the gauge and the rock is critical to the accuracy of the measurement, especially in the case where both loading and unloading conditions would occur at the stressmeter position, the gauge should be preset to 100-200 units above the initial reading as recommended in the installation manual.

(d) Due to the seating adjustment occurring at the stressmeter borehole interface, gradual reduction in the meter reading was noted after installation of the stressmeter but equilibrium condition was reached in about 3 to 4 days. It is recommended that a time allowance be made for the stabilization of the stressmeter reading to take place during the initial part of the monitoring program.

(e) With the use of at least three stressmeters in three conveniently known orientations, the maximum and minimum stress changes on a plane perpendicular to the axis of the borehole may be measured. If similar measurements were made in a second, non-orthogonal borehole, and the initial insitu stresses were known, the new state of stresses with reference to the global co-ordinate system can be determined by the transformation of stresses from the local borehole co-ordinate system.

(f) More information on potential dielectric material for the capacitance type load cells has been obtained and the data are presented in Section 5.

GOLDER ASSOCIATES

Clement M. K. Yuen, P. Eng.

for Guy LeBel

TABLE 1

CALIBRATION TEST PROGRAM

	ASPECT TO BE STUDIED	SCOPE/SPECIAL FEATURE OF TESTING	NO. OF TESTS
1.	Evaluation of the performance of the stressmeter under known uniaxial loading conditions	• conventional axial loading of the block with the stressmeter installed • block pre-loaded at 22.3 to 71.2 kN (5000 to 16000 lbf) • axial load up to 445 kN (100,000 lbf) • varying installation load settings for the stressmeters • 5 VBS-2 stressmeters tested	7
2.	Calibration of the Variation in the response of the stress meter from the axis along which the load is applied	• conventional axial loading of the specimen with the stressmeter installed • angular rotation at 0, 5, 10, 15, 20, 30, 40 and 45° • block pre-loaded at 71.2 kN (16000 lbf) • axial load up to 445 kN (100,000 lbf) • 2 VBS-2 stressmeters tested	16 +4 obtained in aspect No. 1
3.	Evaluation of long term creep	• installation of a stressmeter within a sandstone overcore • monitoring of the changes in reading with time	1

TABLE 2

PHYSICAL PROPERTIES OF PIER CAP SANDSTONE

(a) Physical Properties

Bulk Density	2.19 Mg/m^3	
Porosity	19%	
Gas Permeability	5.22×10^{-6}	cm/s at 5 MPa
	5.24×10^{-6}	cm/s at 10 MPa

(b) Average Strength and Deformation Characteristic

Uniaxial Compressive Strength	43.3 MPa	
Tensile (Brazilian) Strength	4.3 MPa	
Elastic Modulus	10.78 GPa	(1)
Dynamic Modulus (2)	11.95 GPa	

NOTES: (1) Secant modulus at 50% (Based on results of uniaxial compression tests on cylindrical specimens)

(2) Determined from velocities of compressional waves through the sample

TABLE 3

SUMMARY OF TEST CONDITIONS FOR VIBRATING WIRE STRESSMETERS

Stressmeter Serial No.	Test Reference No.	Initial Preload on Block kN (lbf)	Stressmeter Reading Initial	Preset	Diff.
VBS2 (217)	G1-01-0A	71.2 (16000)	2179	2311	132
	G1-10-0B	71.2 (16000)	2176	2250	74
VBS2 (3-29)	T2-01-0A	71.2 (16000)	2082	2127	45
	T2-10-0B	71.2 (16000)	2080	2237	157
VBS2 (10.7)	G2-01-0	22.3 (5000)	2055	2121	66
VBS2 (10.6)	G2-02-0	22.3 (5000)	2110	2226	116
VBS2 (10.51)	G2-03-0	22.3 (5000)	2138	2258	120

Note: Loading area of sandstone block is 14.86×10^3 mm^2.

TABLE 4

CALIBRATION OF STRESSMETER UNDER UNIAXIAL LOADING CONDITIONS

DATA SUMMARY AND REDUCTION[1,2,3]

MEASURED DATA					DATA REDUCTION						
Test Ref. No.	Applied Loading (lbf)	Stressmeter Reading (T) (Units)	Applied Stress Total (psi)	Applied Stress Incremental (psi)	Calculated Stress Change Total (psi)	Calculated Stress Change Incremental (psi)	$\bar{T}$	ΔT	Stressmeter Sensitivity Actual (psi/unit)	Stressmeter Sensitivity Calculated (psi/unit)	$\frac{1}{T^2}$ (1/unit^{2}x10^{-7})
T2-01-0A	16000	2127	694.23	-	-	-	-	-	-	-	2.21
	25000	2155	1084.86	390.63	101.74	101.74	2141	28	13.95	3.63	2.15
	35000	2192	1518.89	434.03	230.75	128.51	2174	37	11.73	3.47	2.08
	50000	2288	2169.93	651.04	535.10	304.84	2240	96	6.78	3.18	1.91
	67000	2475	2907.78	737.85	1030.31	495.21	2382	187	3.95	2.65	1.63
	73000	2576	3168.20	260.42	1254.07	223.76	2526	101	2.58	2.22	1.51
T2-10-0B	16000	2237	694.23	-	-	-	-	-	-	-	2.00
	25000	2313	1084.86	390.63	230.29	230.29	2275	76	5.14	3.03	1.87
	35000	2413	1518.89	434.03	500.78	270.49	2363	100	4.34	2.70	1.72
	50000	2616	2169.93	651.04	957.57	456.79	2515	203	3.21	2.25	1.46
	67000	2931	2907.78	737.85	1487.46	529.89	2774	315	2.34	1.68	1.16
	84000	3398	3645.83	737.85	2018.71	531.25	3165	467	1.58	1.14	0.87
	100000	4075 [4]	4340.27	694.44	2489.15	470.44	3737	677	1.03	0.69	0.60
G1-01-0A	16000	2311	694.23	-	-	-	-	-	-	-	1.87
	25000	2418	1084.86	390.63	288.91	288.91	2365	107	3.65	2.70	1.71
	35000	2559	1518.89	434.03	615.69	326.78	2489	141	3.08	2.32	1.53
	50000	2851	2169.93	651.04	1144.84	529.14	2705	292	2.23	1.81	1.23
	67000	3363	2907.78	737.85	1761.89	617.05	3107	512	1.44	1.21	0.88
	84000	4245 [4]	3645.63	737.85	2348.91	587.02	3804	882	0.84	0.67	0.55
G1-10-0B	16000	2250	694.23	-	-	-	-	-	-	-	1.98
	25000	2319	1084.86	390.63	206.46	206.46	2285	69	5.66	2.99	1.86
	35000	2424	1518.89	434.03	487.45	281.00	2372	105	4.13	2.68	1.70
	50000	2640	2169.93	651.04	963.67	476.21	2532	216	3.01	2.20	1.44
	67000	2986	2907.78	737.85	1522.16	558.49	2813	346	2.13	1.61	1.12
	84000	3533	3645.63	737.85	2093.41	571.25	3260	547	1.35	1.04	0.80
	60000	2870	2604.17	-1041.46	1357.25	-736.16	3202	-663	1.57	1.15	1.21
	40000	2484	1736.11	- 868.06	632.27	-724.98	2677	-386	2.25	1.88	1.62
	20000	2255	868.05	- 868.06	15.60	-616.67	2370	-229	3.79	2.69	1.97
	0	2162	0	- 868.06	-292.55	-308.13	2209	- 93	9.33	3.31	2.14

NOTE: 1. Units shown are imperial units conforming to manufacturers calibration
2. Conversion factors are 1 lbf = 4.448 kN 1 psi = 6.895 kPa
3. Applied stresses are calculated based on a loading area of 14.86 x 10^3 mm^2 (23.04 in^2)
4. The stress meter upper limit range is 4000 units.

Golder Associates

TABLE 4 (Cont'd)

MEASURED DATA					DATA REDUCTION						
Test Ref. No.	Applied Loading (lbf)	Stressmeter Reading (T) (Units)	Applied Stress Total (psi)	Applied Stress Incremental (psi)	Calculated Stress Change Total (psi)	Calculated Stress Change Incremental (psi)	$\bar{T}$	ΔT	Stressmeter Sensitivity Actual (psi/unit)	Stressmeter Sensitivity Calculated (psi/unit)	$\frac{1}{T^2}$ (1/unit^{2}x10^{-7})
G2-01-0	5000	2121	217.01	-	-	-	-	-	-	-	2.22
	10000	2150	434.03	217.01	106.19	106.19	2136	29	7.48	3.66	2.16
	20000	2228	868.06	434.03	371.52	265.33	2189	78	5.56	3.40	2.01
	30000	2354	1302.09	434.03	745.73	374.20	2291	126	3.44	2.97	1.80
	40000	2513	1736.12	434.03	1139.99	394.26	2434	159	2.73	2.48	1.58
	50000	2675	2170.15	434.03	1471.59	331.60	2594	162	2.68	2.05	1.40
	60000	2925	2604.18	434.03	1879.30	407.71	2800	250	1.74	1.63	1.17
	70000	3240	3038.21	434.03	2264.81	385.20	3083	315	1.38	1.22	0.95
	80000	3642	3472.24	434.03	2648.09	383.29	3461	402	0.98	0.87	0.74
	90000	4379 (a)	3906.27	434.03	3033.42	395.33	4031	737	0.62	0.55	0.52
	75000	3451	3255.23	-651.04	2466.14	-567.28	3915	-928	0.70	0.61	0.84
	55000	2775	2387.17	-868.06	1647.93	-818.21	3113	-676	1.28	1.21	1.30
	35000	2407	1519.11	-868.06	885.86	-762.07	2591	-368	2.36	2.07	1.73
	15000	2146	651.05	-868.06	91.80	-794.06	2277	-261	3.33	3.04	2.17
	5000	2056	217.02	-434.03	-254.55	-346.45	2101	- 90	4.82	3.85	2.37
	0	2040	0	-217.01	-320.97	- 66.42	2048	- 16	13.56	4.17	2.40
G2-02-0	5000	2226	217.01	-	-	-	-	-	-	-	2.02
	10000	2289	434.03	217.01	195.34	195.34	2258	63	3.44	3.10	1.91
	20000	2454	868.06	434.03	637.54	442.20	2372	165	2.63	2.68	1.66
	30000	2655	1302.09	434.03	1068.84	431.30	2555	201	2.16	2.15	1.42
	40000	2931	1738.12	434.03	1522.76	453.92	2793	276	1.57	1.64	1.16
	50000	3266	2170.15	434.03	1926.67	403.91	3099	335	1.30	1.21	0.94
	60000	3691	2604.18	434.03	2289.43	362.76	3479	425	1.02	0.85	0.73
	65000	4053 (a)	2821.19	217.01	2512.77	223.34	3872	362	0.60	0.62	0.61
	55000	3444	2387.16	-434.03	2094.98	-417.78	3749	-609	0.71	0.69	0.84
	35000	2761	1519.10	-868.06	1259.32	-835.66	3103	-683	1.27	1.22	1.31
	15000	2320	651.04	-868.06	285.67	-973.66	2541	-441	1.97	2.21	1.86
	5000	2162	217.01	-434.03	-216.18	-501.84	2241	-158	2.75	3.18	2.14
	0	2115	0	-217.01	-387.59	-171.41	2139	- 47	4.62	3.65	2.24
G2-03-0	5000	2258	217.01	-	-	-	-	-	-	-	1.96
	10000	2329	434.03	217.01	209.96	209.96	2294	71	3.06	2.96	1.84
	20000	2469	868.05	434.03	572.14	362.19	2399	140	3.10	2.59	1.64
	30000	2644	1302.08	434.03	946.49	374.35	2557	175	2.48	2.14	1.43
	40000	2838	1736.11	434.03	1283.25	336.76	2741	194	2.24	1.74	1.24
	50000	3090	2170.14	434.03	1629.58	346.43	2964	252	1.72	1.37	1.05
	60000	3378	2604.17	434.03	1934.41	304.83	3234	288	1.51	1.06	0.86
	70000	3804	3038.20	434.03	2264.76	330.06	3591	426	1.02	0.78	0.69
	80000	4412 (b)	3472.23	434.03	2580.95	316.18	4108	608	0.71	0.52	0.51
	65000	3471	2821.19	-651.04	2017.01	-563.93	3942	-941	0.69	0.60	0.83
	55000	3093	2387.16	-434.03	1633.20	-383.81	3282	-378	1.15	1.02	1.05
	35000	2599	1519.10	-868.06	857.41	-775.79	2846	-494	1.76	1.57	1.48
	15000	2270	651.04	-868.06	36.87	-820.54	2435	-329	2.64	2.49	1.94
	5000	2161	217.01	-434.03	-320.97	-357.84	2216	-109	3.98	3.28	2.14
	0	2128	0	-217.01	-440.30	-119.33	2145	- 33	6.50	3.62	2.21

Golder Associates

TABLE 5

TYPICAL STRAIN MEASUREMENTS DURING CALIBRATION OF STRESS METER UNDER UNIAXIAL LOADING CONDITIONS

Applied Stress psi	Applied Stress MPa	Strain Gauges Readings in the Central Half of the Sandstone Block #2	#3	#6	#7
0.00	0.0	0	0	0	0
217.01	1.5	-32[1]	- 40	4	- 4
434.03	3.0	-82	-212	-196	-204
868.06	6.0	-360	-526	-490	-530
1302.08	9.0	-644	-798	-738	-806
1736.11	12.0	-888	-1018	-946	-1032
2170.14	15.0	-1062	-1178	-1092	-1196
2604.17	18.0	-1260	-1360	-1268	-1384
3038.19	21.0	-1440	-1528	-1430	-1600
3472.22	23.9	-1614	-1688	-1582	-1728
3906.25	26.9	-1800	-1858	-1738	-1894
3255.21	22.4	-1610	-1672	-1564	-1712
2387.15	16.5	-1280	-1348	-1272	-1406
1519.10	10.5	- 914	-1004	- 958	-1062
651.04	4.5	- 388	- 514	- 490	- 562
217.01	1.5	- 46	- 110	- 68	- 86
0.00	0.0	- 8	198	284	264
0.00	0.0	32	262	284	284

NOTE: (1) Negative values indicate compression

TABLE 6

COMPARISON OF ACTUAL AND THEORETICAL SLOPES IN THE STRESS VS $\frac{1}{T^2}$ RELATIONSHIPS

Theoretical Slope: 17.82×10^{11}

Test No.	Actual Slope ($\times 10^{11}$)	$\left(\frac{\text{Actual-Theoretical}}{\text{Actual}}\right) \times 100$
T2-01-0A	20.8	14.3
T2-10-0B	24.3	26.7
G1-01-0A	22.3	20.1
G1-10-0B	23.6	24.5
G2-01-0	19.8	10.0
G2-02-0	16.8	-6.1
G2-03-0	19.4	8.1

TABLE 7

EFFECTS OF ANGULAR ROTATION ON STRESS CHANGE MEASUREMENTS

Stressmeter Serial No.	Test No.	Angle (σ)	Change in stressmeter readings due to change in load from 67000 to 84000 (lbf)	Calculated stress change (psi) σ_r	$\frac{\sigma_r}{\sigma_{ro}}$ (%)	Remarks
VBS2 (217)	G1-01-0A	0°	882	587.02	100	σ_r/σ_{ro} calculated based on σ_{ro} = 579.14 psi
	G1-10-0B	0°	547	571.25		
				Av = 579.14 (σ_{ro})		
	G1-02-05	5°	819	520.44	90	
	G1-03-10	10°	830	495.96	85	
	G1-04-15	15°	703	405.90	70	
	G1-05-20	20°	228	335.07	58	
	G1-06-30	30°	62	126.70	22	
	G1-07-45	45°	-6	18.61	-	
VBS2 (3-29)	T2-10-0B	0°	467	531.25(σ_{ro})	100	σ_r/σ_{ro} calculated based on σ_{ro} = 531.25 psi
	T2-02-05	5°	368	517.25	98	
	T2-03-10	10°	280	450.29	85	
	T2-04-20	20°	171	363.61	68	
	T2-05-30	30°	50	134.98	25	
	T2-06-40	40°	6	20.12	3.8	
	T2-07-45	45°	-6	-20.01	-	

1. Calculated stress changes are based on equation (1) in section 3.3.2

2. Units shown are imperial units conforming to manufacturer's calibration.

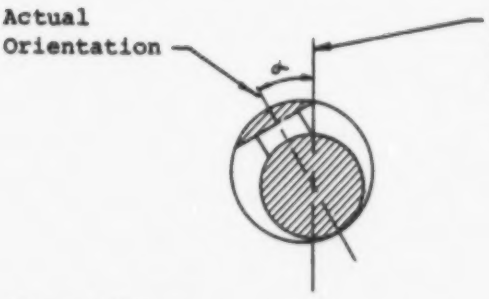

TABLE 8

EVALUATION OF LONG TERM CREEP

DATE/TIME	ELAPSED TIME (min)	METER READINGS	DIFFERENCE FROM INITIAL READING	REMARKS
March 21,85/ -	-	2087		
March 21,85/11:17 hr.	0	2227 (T_o)	0	Initial reading (Stressmeter pre-loaded in specimen)
March 21,85/11:18 hr.	1	2226	-1	
March 21,85/11:23 hr.	6	2225	-2	
March 21,85/11:28 hr.	11	2225	-2	
March 21,85/15:28 hr.	251	2219	-8	
March 21,85/16:00 hr.	283	2218	-9	
March 22,85/10:42 hr.	1405	2214	-13	
March 22,85/15:17 hr.	1680	2212	-15	
March 26,85/8:56 hr.	7059	2206	-21	
March 27,85/8:28 hr.	8471	2206	-21	
March 27,85/15:04 hr.	8867	2206	-21	

NOTE: Creep test carried out in a sandstone overcore with no externally applied stresses.

STRESSMETER UNIAXIAL SENSITIVITY (SR) | FIGURE 1

Date MAR. 29, 1985
Project 841-1251

Golder Associates

Drawn G.P.
Chkd.

STRESSMETER UNIAXIAL SENSITIVITY (SR) | FIGURE 2

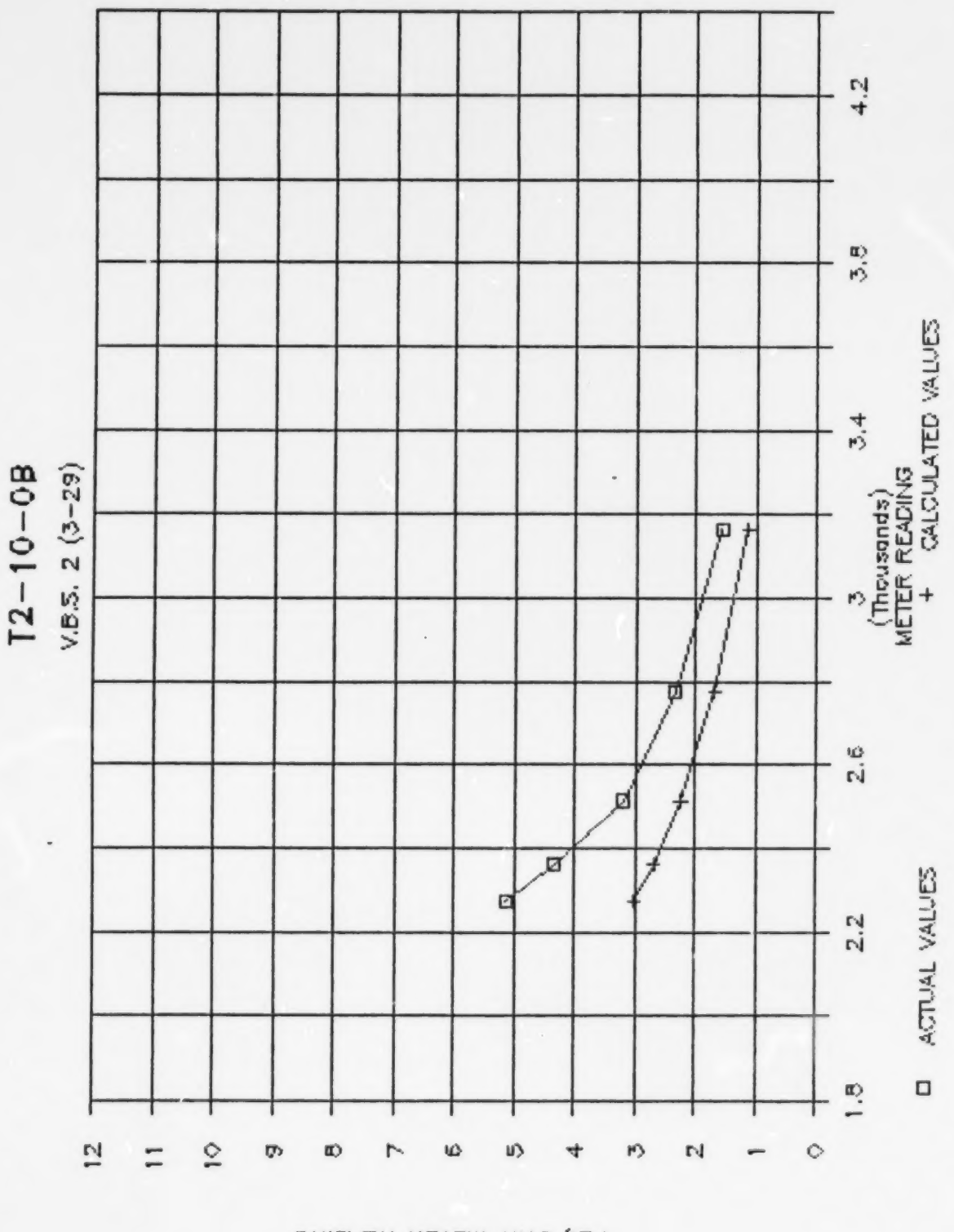

Date MAR. 29,1985
Project 841-1251

Golder Associates

Drawn G.P.
Chkd.

STRESSMETER UNIAXIAL SENSITIVITY (SR) | FIGURE 3

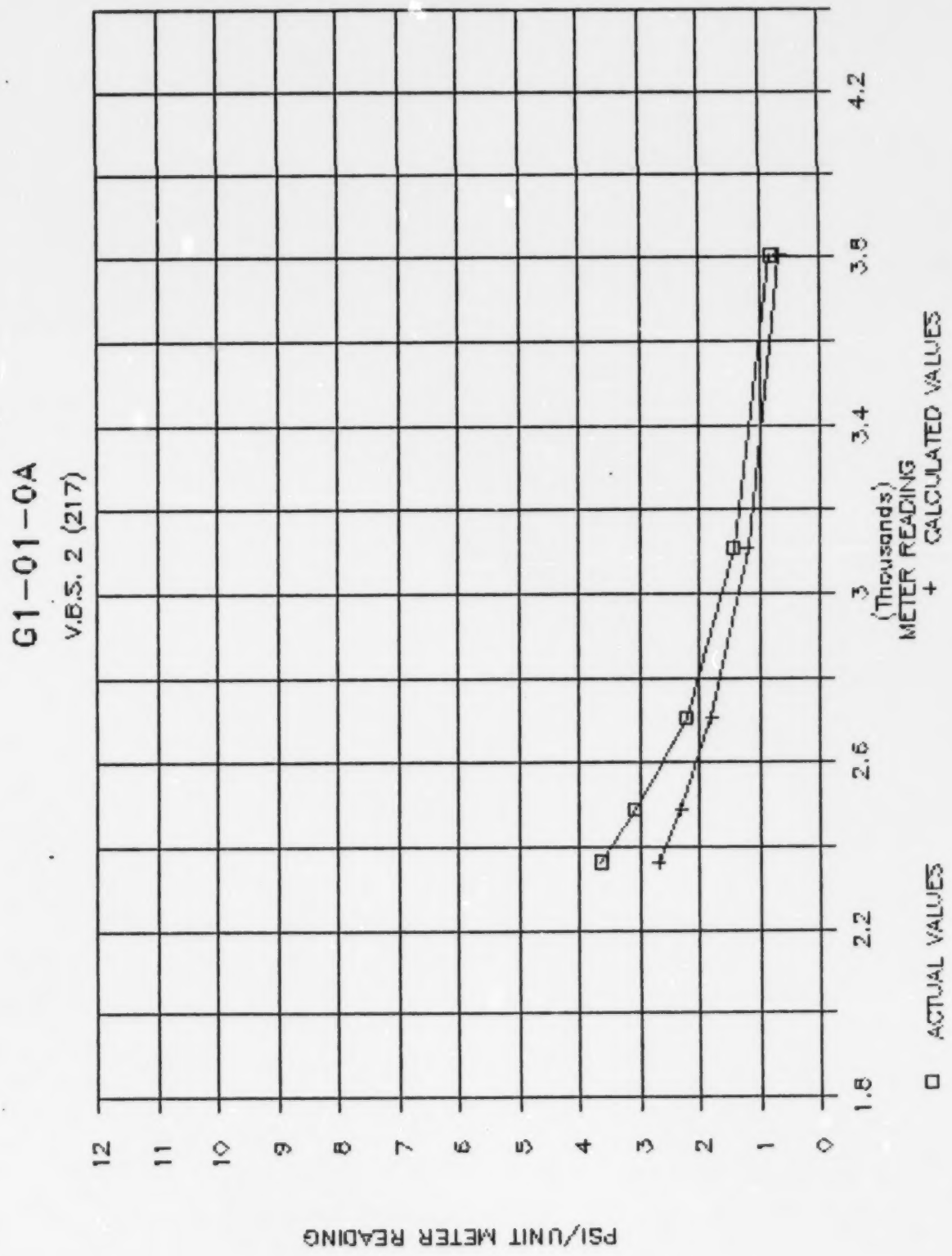

Date MAR. 29, 1985
Project 841-1251

Golder Associates

Drawn G.P.
Chkd.

STRESSMETER UNIAXIAL SENSITIVITY (SR)

FIGURE 4

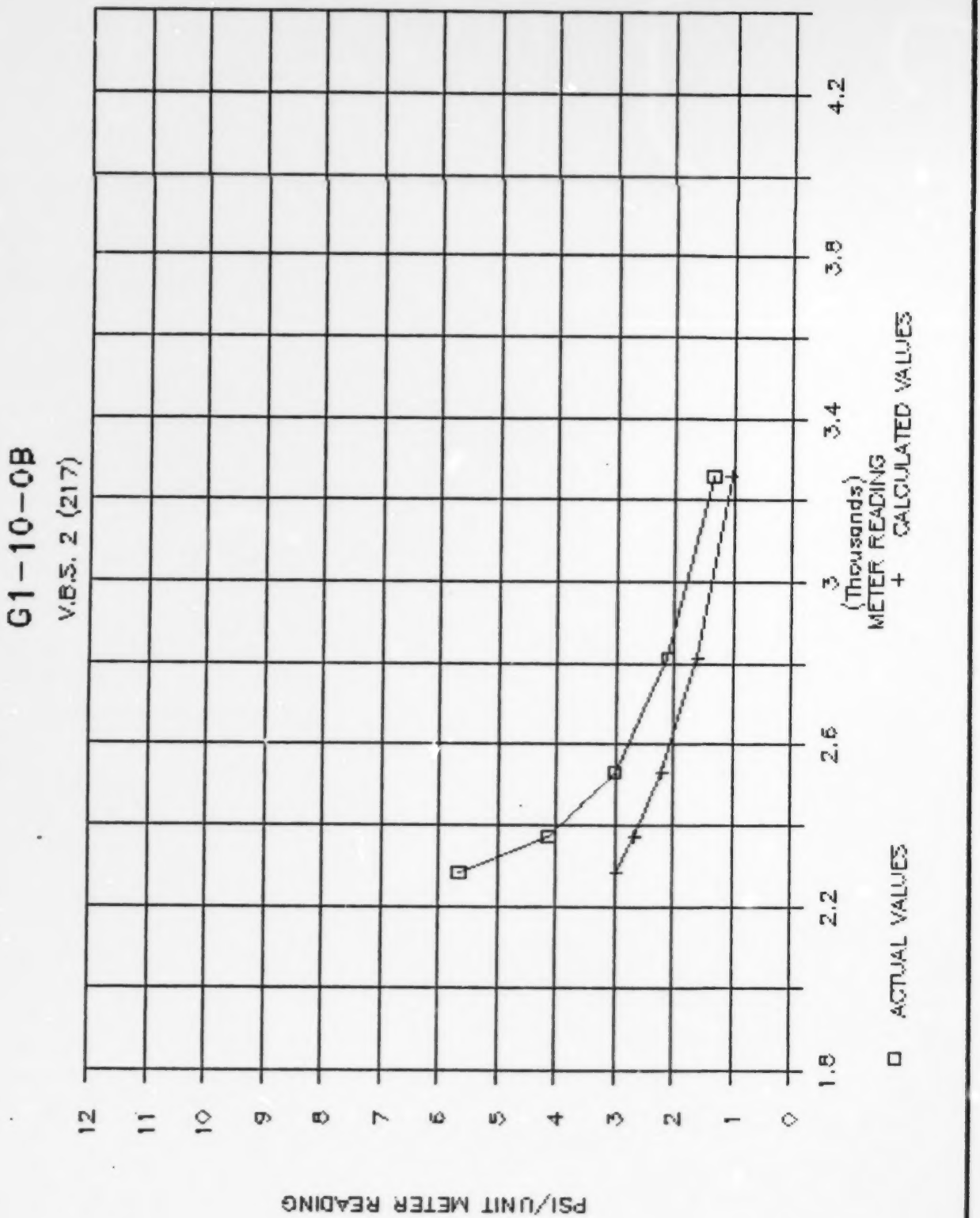

Date MAR. 29,1985

Project 841-1251

Golder Associates

Drawn G.P.

Chkd.

STRESSMETER UNIAXIAL SENSITIVITY (SR)

FIGURE 5

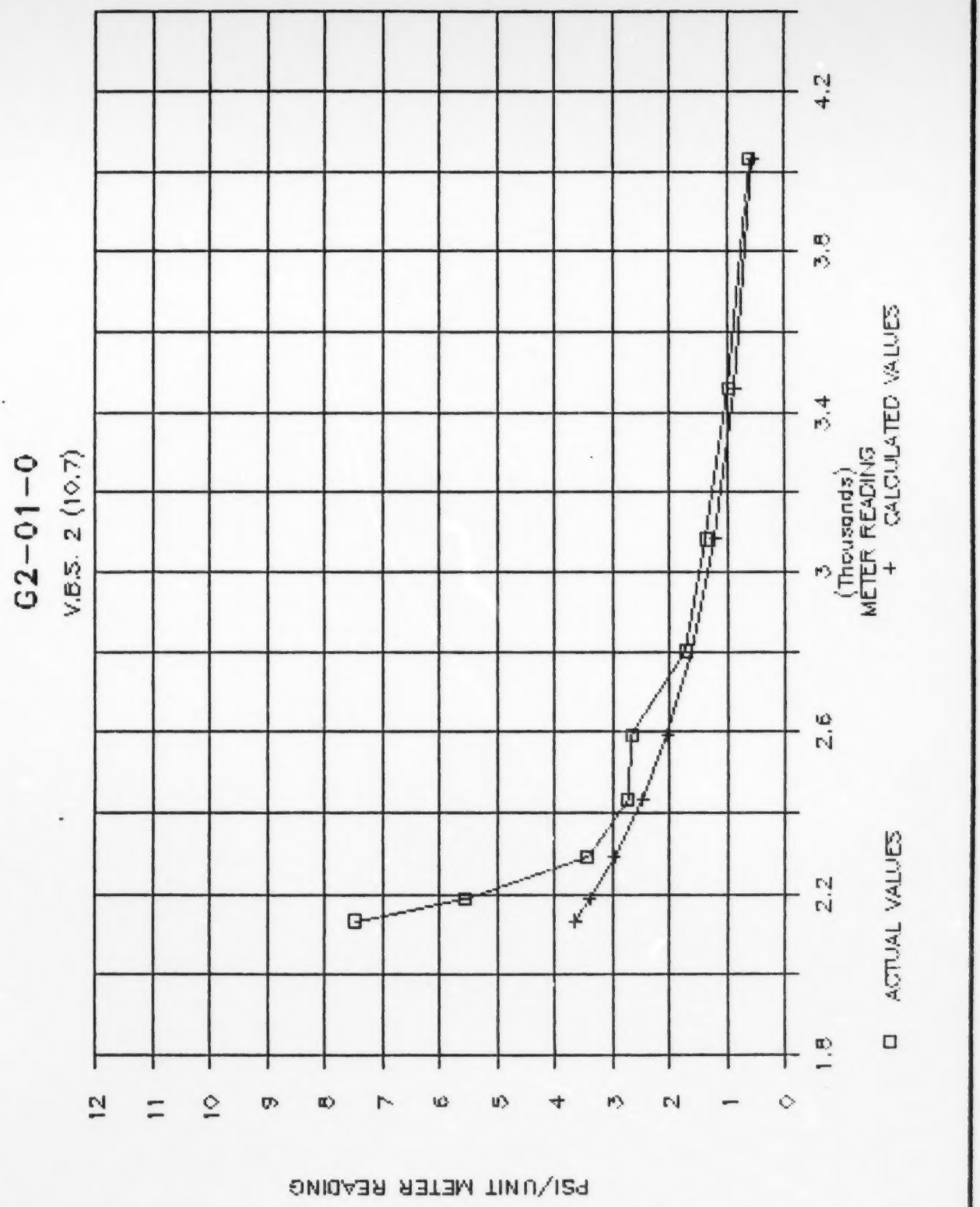

Date MAR. 29,1985

Project 841-1251

Golder Associates

Drawn G.P.

Chkd.

STRESSMETER UNIAXIAL SENSITIVITY (SR)

FIGURE 6

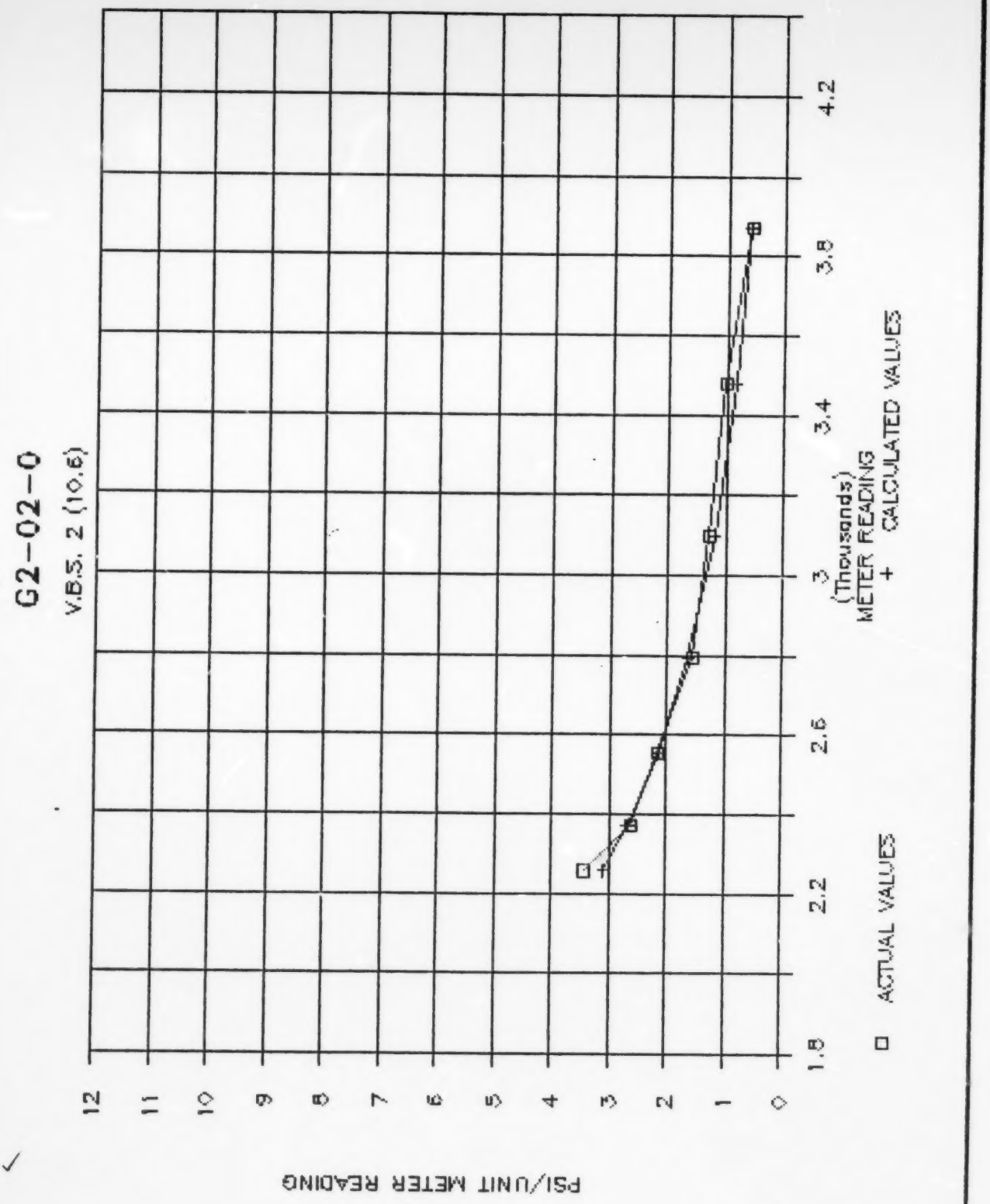

Date MAR. 29,1985

Project 841-1251

Golder Associates

Drawn G.P.

Chkd.

STRESSMETER UNIAXIAL SENSITIVITY (SR)

FIGURE 7

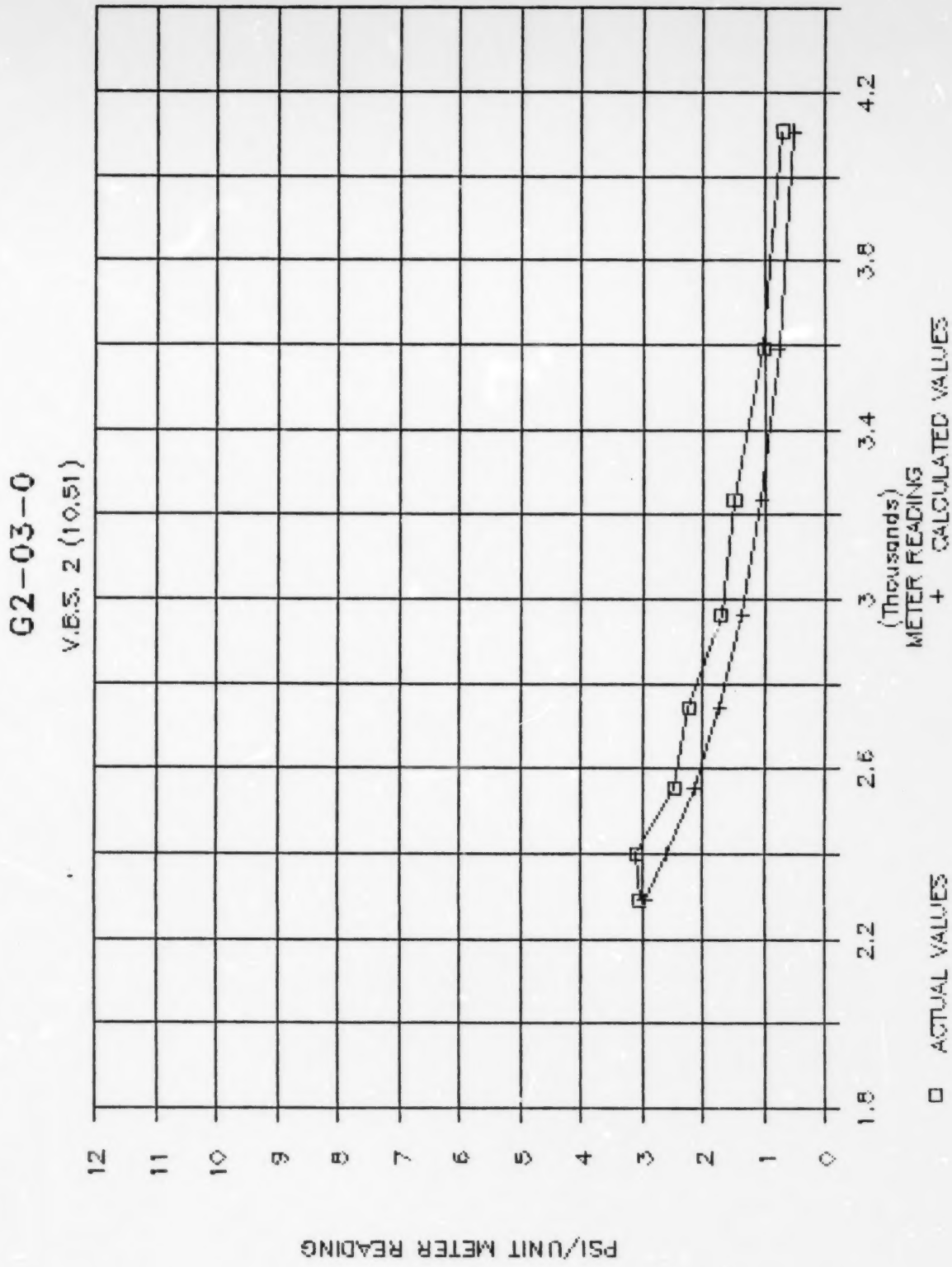

Date MAR. 29,1985

Project 841-1251

Golder Associates

Drawn G.P.

Chkd.

APPLIED STRESS VERSUS $\frac{1}{T^2}$

FIGURE 8

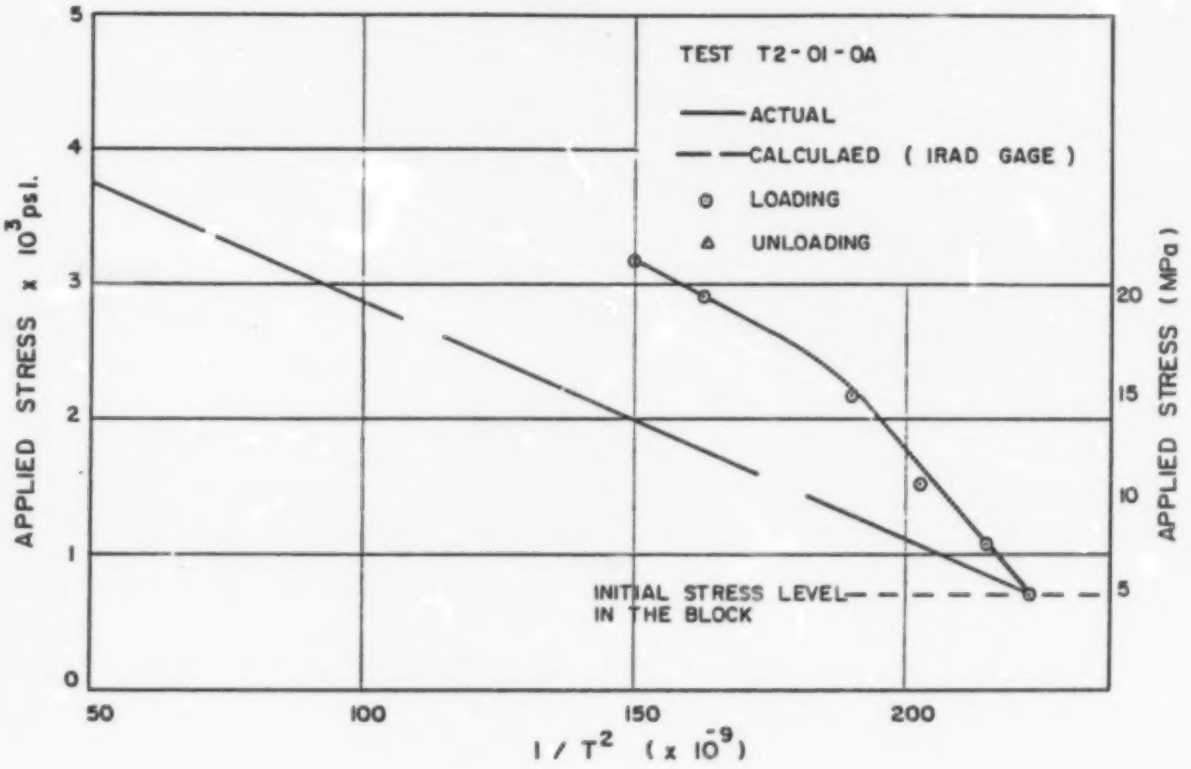

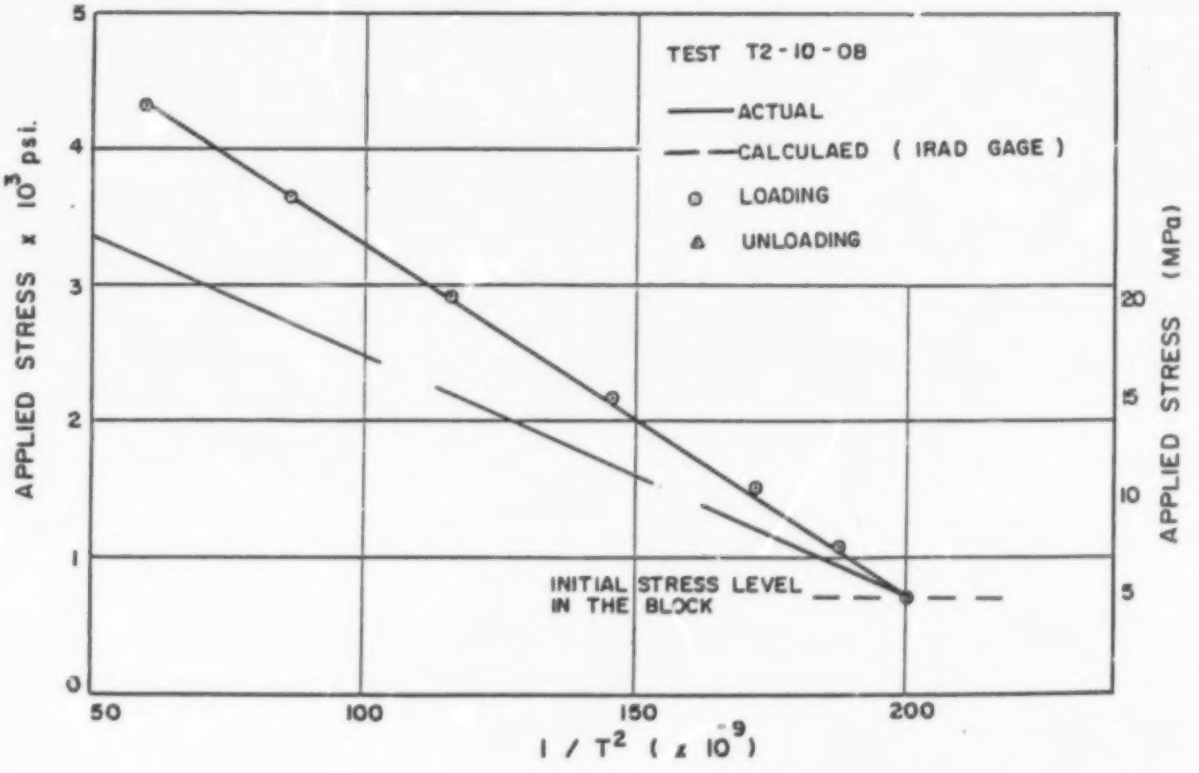

Date MAR. 29, 1985

Project 841-1251

Golder Associates

Drawn G.P.

Chkd.

APPLIED STRESS VERSUS $\frac{1}{T^2}$

FIGURE 9

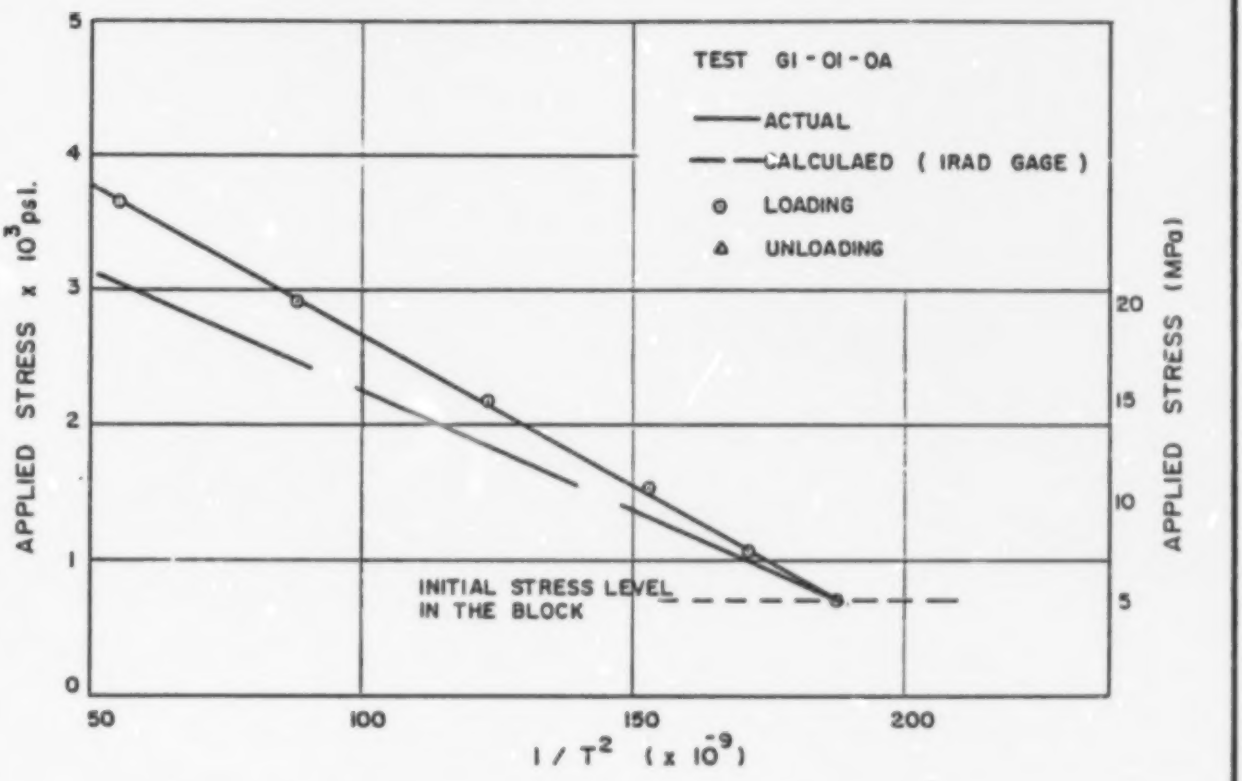

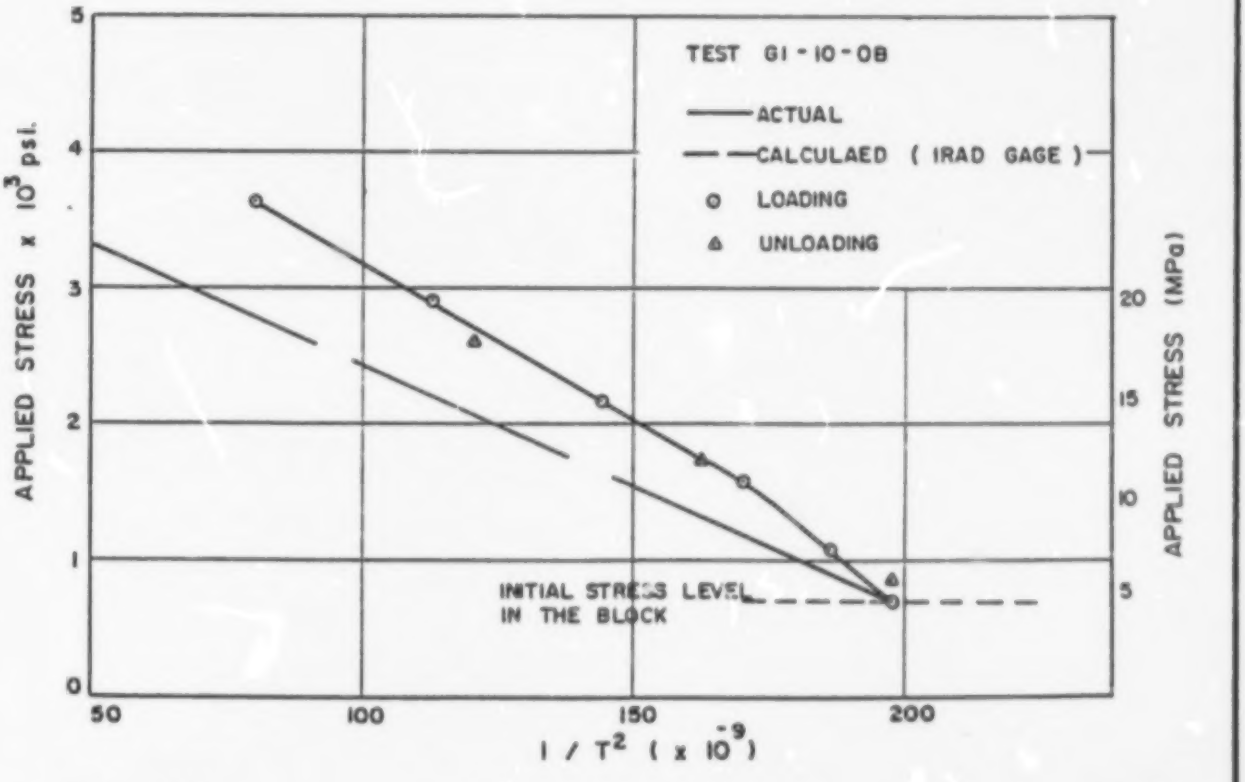

Date MAR. 29, 1985
Project 841-1251

Golder Associates

Drawn G.
Chkd.

APPLIED STRESS VERSUS $\frac{1}{T^2}$

FIGURE 10

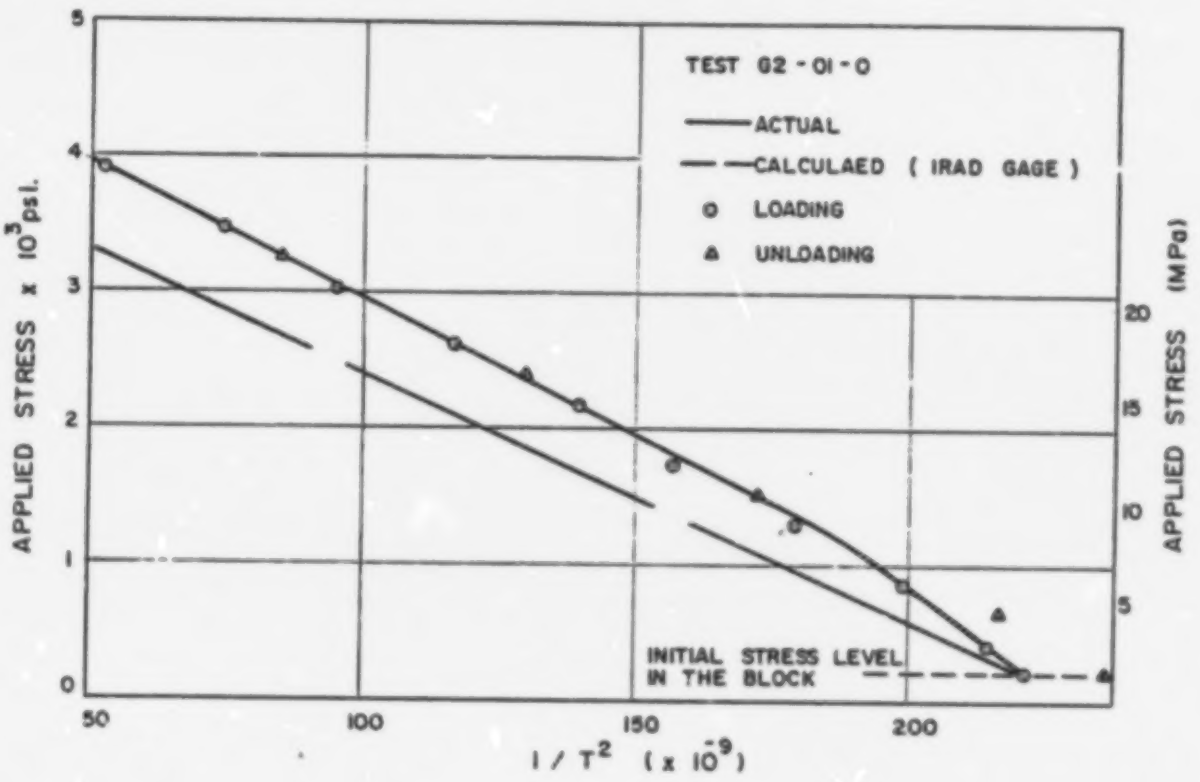

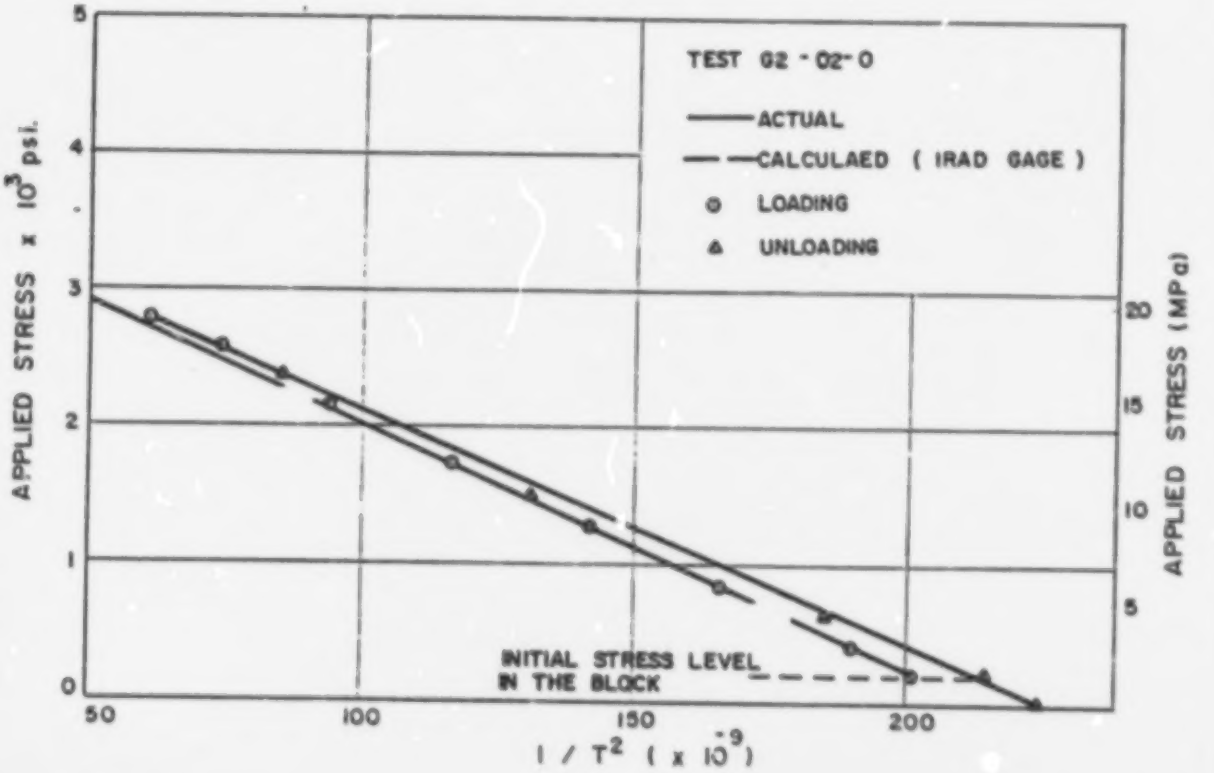

Date MAR. 29, 1985

Project 841-1251

Golder Associates

Drawn G.P.

Chkd.

APPLIED STRESS VERSUS $\frac{1}{T^2}$

FIGURE 11

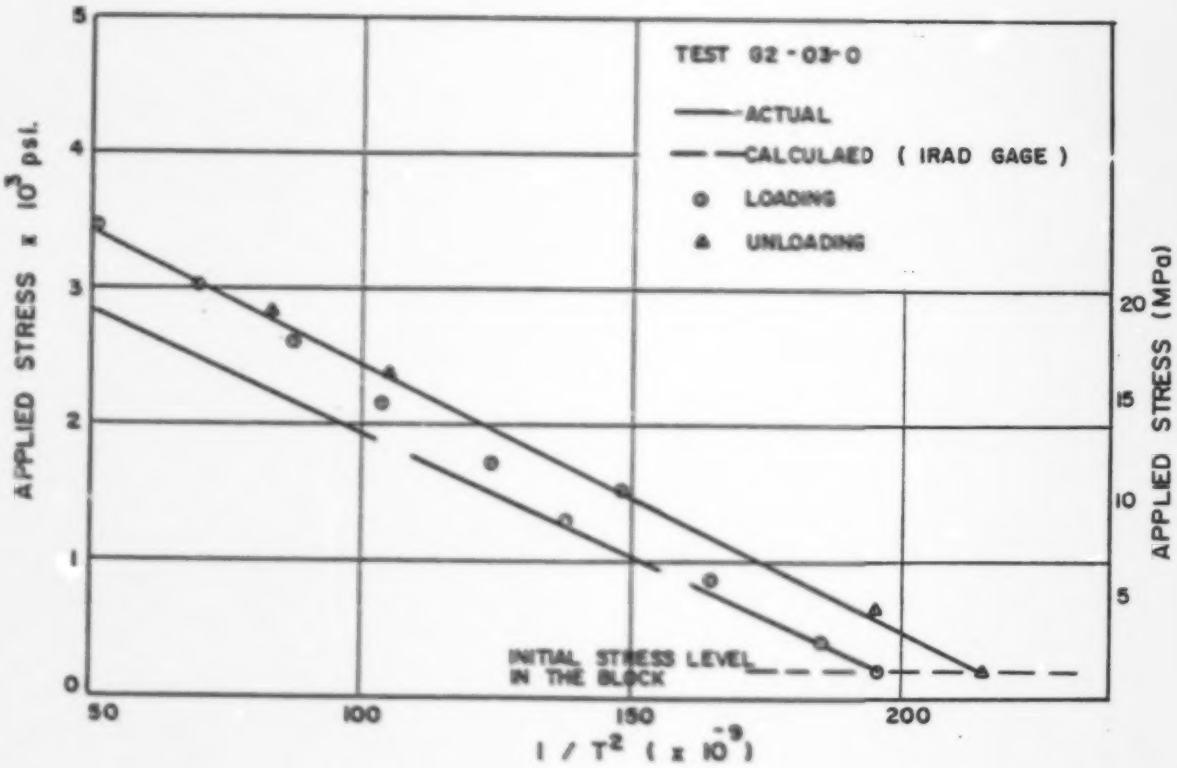

Date MAR.29,1985

Project 841-125

Golder Associates

Drawn G.P.

Chkd.

EFFECT OF STRESSMETER INSTALLATION ANGLE ON MEASURED STRESS CHANGES

FIGURE 12

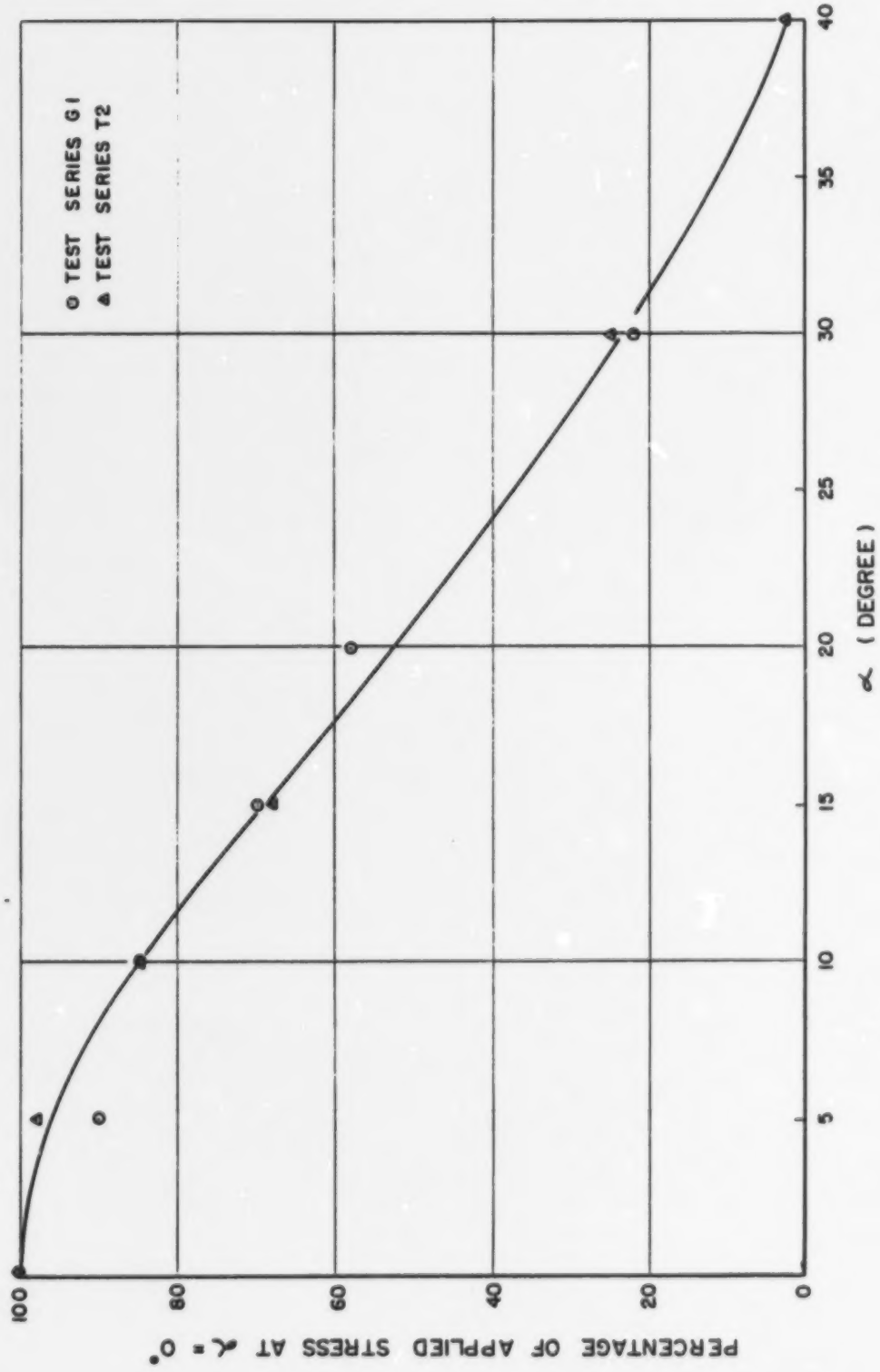

Date MAR. 29, 1985
Project 841-1251

Golder Associates

Drawn G.P.
Chkd.

CO-ORDINATE SYSTEMS FOR EVALUATION OF INSITU STRESSES

FIGURE 13

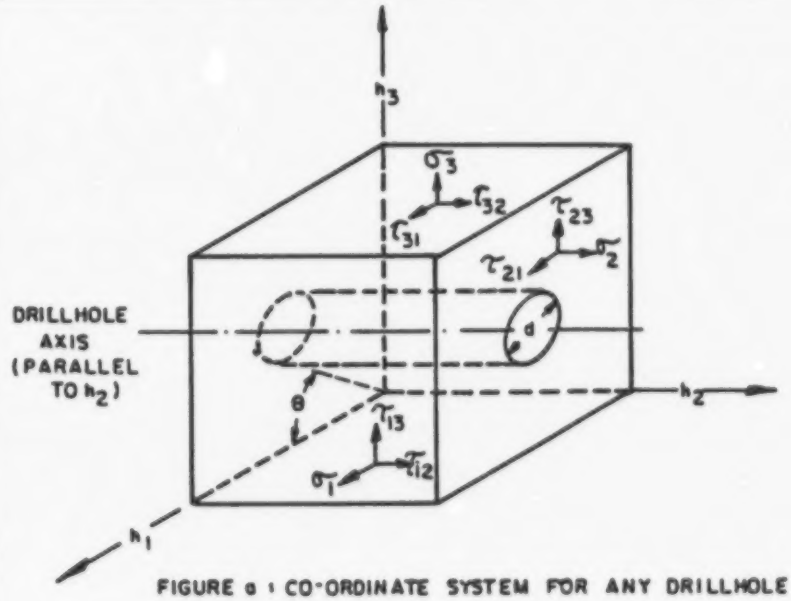

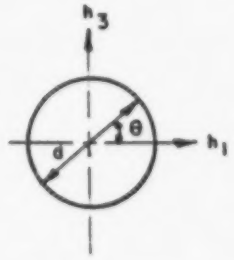

θ = ORIENTATION OF DIAMETRAL DEFORMATION (MEASURED FROM h_1 AXIS)

FIGURE a : CO-ORDINATE SYSTEM FOR ANY DRILLHOLE

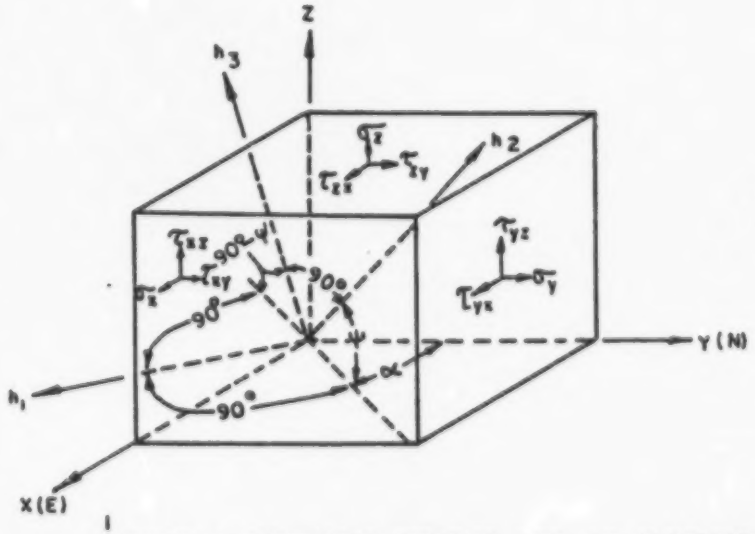

FIGURE b : CO-ORDINATE SYSTEMS FOR AN ARBITRARILY ORIENTED DRILL HOLE IN AN x, y, z CO-ORDINATE SYSTEM (x - EAST, y - NORTH, AND z - VERTICAL)

α - AZIMUTH OF DRILL HOLE

ψ - INCLINATION OF DRILL HOLE

NOTES

ALL CO-ORDINATE AXES ARE SHOWN IN THEIR POSITIVE DIRECTIONS.

Date MAR. 29, 1985
Project No. 841-1251

Golder Associates

Drawn D.M.
Chkd.

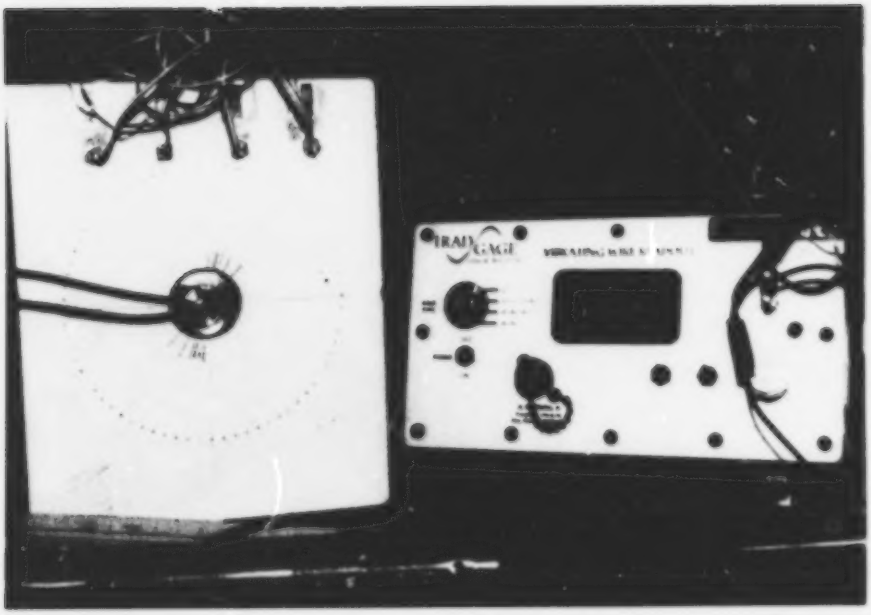

PLATE 1: Readout unit, stressmeter and instrumented sandstone block

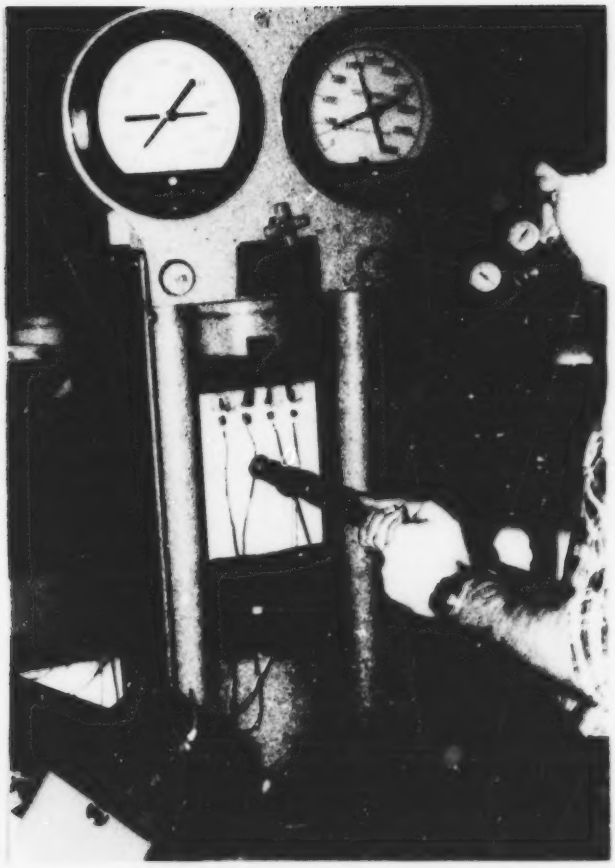

PLATE 2: Installation of the stressmeter in the preloaded sandstone block

APPENDIX A

COMPUTATION OF NEW PRINCIPAL STRESSES FROM MEASURED STRESS CHANGES

APPENDIX A

COMPUTATION OF NEW PRINCIPAL STRESS FROM MEASURED STRESS CHANGES

The local and global co-ordinate systems for the computation of stress changes and new principal stresses are defined in Figure 13 . The procedures of computations are outlined below.

(a) Determination of Stress Changes on h_1, h_3 Plane

The orientation and the magnitudes of the principal stress changes (P, Q) in the h_1, h_3 plane (plane perpendicular to the borehole axis) can be determined by undertaking 3 uniaxial stress change measurements, one each in the direction of h_1 and h_3, and one at 45° to h_1. The stress changes and β are given in Irad Gage's manual and presented below.

$$P = \frac{3}{2} a + \frac{3}{4} b \qquad (A1)$$

$$Q = \frac{3}{2} a - \frac{3}{4} b \qquad (A2)$$

$$\beta = \frac{1}{2} \sin^{-1} \frac{\Delta\sigma_{45}}{b} \qquad (A3)$$

where; $a = \frac{\Delta\sigma_3 + \Delta\sigma_1}{2}$ (A4)

$$b = [(\Delta\sigma_{45}-a)^2 + (\Delta\sigma_3-a)^2]^{\frac{1}{2}} \qquad (A5)$$

$\Delta\sigma_1$, $\Delta\sigma_3$ = stress changes measured in the h_1 and h_3 axes respectively

$\Delta\sigma_{45}$ = stress change measured in the direction at 45° to the h_1 axis

P, Q = maximum and minimum stress changes

β = angle between the h_3 axis and the direction of the maximum principal stress change measured anticlockwise

(b) Determination of New Absolute Stresses on h_1, h_3 Plane

Based on the measured stress changes and the initial stresses, the new absolute stresses with reference to the h_1, h_2, h_3 co-ordinate system can be evaluated:

$$\begin{aligned} \sigma_1 &= \sigma_{1i} + \Delta\sigma_1 \\ \sigma_3 &= \sigma_{3i} + \Delta\sigma_3 \\ \tau_{31} &= \tau_{31i} + \Delta\tau_{31} \end{aligned} \qquad \text{(A6)}$$

where; $\sigma_1, \sigma_3, \tau_{31}$ = new absolute stress components

$\sigma_{1i}, \sigma_{3i}, \tau_{31i}$ = initial absolute stress components

$\Delta\sigma_1, \Delta\sigma_3, \Delta\tau_{31}$ = changes in the stress components

$$\Delta\tau_{31} = \frac{\Delta\sigma_1 - \Delta\sigma_3}{2} \sin 2\beta$$

If the stress changes were again measured in a second non-orthogonal borehole, similar calculation can be made for the new absolute stresses in the local borehole co-ordinate system.

The new absolute stresses measured in the borehole can be related to the six stress components (σ_x, σ_y, σ_z, τ_{xy}, τ_{yz} and τ_{yx}) which are referenced to a global co-ordinate system (x,y,z) which could be the mine grid or an arbitrary but convenient system of reference.

The formulae for the transformation of stresses in three-dimensions may be written as:

$$\begin{bmatrix} \sigma_1 \\ \sigma_2 \\ \sigma_3 \\ \tau_{12} \\ \tau_{23} \\ \tau_{31} \end{bmatrix} = \begin{bmatrix} \ell_1^2 & m_1^2 & n_1^2 & 2\ell_1 m_1 & 2m_1 n_1 & 2n_1 \ell_1 \\ \ell_2^2 & m_2^2 & n_2^2 & 2\ell_2 m_2 & 2m_2 n_2 & 2n_2 \ell_2 \\ \ell_3^2 & m_3^2 & n_3^2 & 2\ell_3 m_3 & 2m_3 n_3 & 2n_3 \ell_3 \\ \ell_1\ell_2 & m_1 m_2 & n_1 n_2 & (\ell_1 m_2 + \ell_2 m_1) & (m_1 n_2 + m_2 n_1) & (n_1 \ell_2 + n_2 \ell_1) \\ \ell_2\ell_3 & m_2 m_3 & n_2 n_3 & (\ell_2 m_3 + \ell_3 m_2) & (m_2 n_3 + m_3 n_2) & (n_2 \ell_3 + n_3 \ell_2) \\ \ell_1\ell_3 & m_1 m_3 & n_1 n_3 & (\ell_1 m_3 + \ell_3 m_1) & (m_1 n_3 + m_3 n_1) & (n_1 \ell_3 + n_3 \ell_1) \end{bmatrix} \times \begin{bmatrix} \sigma_x \\ \sigma_y \\ \sigma_z \\ \tau_{xy} \\ \tau_{yz} \\ \tau_{zx} \end{bmatrix} \qquad \text{(A7)}$$

ℓ_1, m_1, n_1 are the direction cosines for the positive h_1 axis with the positive X, Y, Z axis. For a given azimuth of drillhole orientation, α, and dip of drillhole (uphole), Ψ, the direction cosines are given by the following relationships:

$$\begin{vmatrix} \ell_1 & \ell_2 & \ell_3 \\ m_1 & m_2 & m_3 \\ n_1 & n_2 & n_3 \end{vmatrix} = \begin{vmatrix} \cos\alpha & \sin\alpha\cos\Psi & -\sin\alpha\sin\Psi \\ -\sin\alpha & \cos\alpha\cos\Psi & -\cos\alpha\sin\Psi \\ 0 & \sin\Psi & \cos\Psi \end{vmatrix} \quad \text{(A8)}$$

The six stress components ($\sigma_x, \sigma_y, \sigma_z, \tau_{xy}, \tau_{yz}, \tau_{zx}$) can be solved if six independent equations can be set-up from A7. Once these components are determined, the new principal stresses can be evaluated.

(c) Determination of New Principal Stresses

With the six independent components of the stress tensor determined with respect to the X, Y, Z, co-ordinate system, it is possible to calculate the stress components with respect to any other cartesian co-ordinates. One transformation which will be of interest is the evaluation of the principal stresses and their directions from the six stress components.

If S_1, S_2, and S_3 are defined as the three principal stress components, there is a set of co-ordinate axes, 1, 2 and 3 such that the shear stresses $S_{12} = S_{23} = S_{31} = 0$. These axes are then the principal stress axes, the formulae for determining the principal stresses and their directions are given below.

The principal stresses are the three roots of the following cubic equation.

$$S^3 + 3BS^2 + 3CS + D = 0 \qquad \text{(A9)}$$

where

$$B = -(\sigma_x^* + \sigma_y + \sigma_z)/3, \qquad \text{(A10)}$$

$$C = (\sigma_x\sigma_y + \sigma_y\sigma_z + \sigma_z\sigma_x - \tau_{xy}^2 - \tau_{yz}^2 - \tau_{zx}^2)/3,$$

and $$D = -\sigma_x\sigma_y\sigma_z - 2\tau_{xy}\tau_{yz}\tau_{zx} + \sigma_x\tau_{yz}^2 + \sigma_y\tau_{zx}^2 + \sigma_z\tau_{xy}^2$$

* compressive stresses are taken as -ve in this formulation

The three roots S_1, S_2, S_3 of equations 8 are found by calculating:

$$\begin{aligned} E &= (B^2 - C)^{\frac{1}{2}}, \\ F &= -B^3 + (3BC - D)/2, \\ \cos 3A &= \pm F/E^3, \qquad \text{(A11)} \\ S_1 &= -B \pm 2E \cos A, \\ S_2 &= -B \pm 2E \cos (A + 120°), \\ S_3 &= -B \pm 2E \cos (A + 240°), \end{aligned}$$

(where ± appears, use + if F is positive, use - if F is negative)

The direction cosines for principal direction 1 with respect to x, y, z are found from the following equations:

$$\begin{aligned} (S_1 - \sigma_x)\, l_1' - \tau_{xy} m_1' - \tau_{zx} n_1' &= 0, \\ -\tau_{xy} l_1' + (S_1 - \sigma_y) m_1' - \tau_{yz} n_1' &= 0, \qquad \text{(A12)} \\ -\tau_{zx} l_1' - \tau_{yz} m_1' + (S_1 - \sigma_z) n_1' &= 0, \\ (l_1')^2 + (m_1')^2 + (n_1')^2 &= 1 \end{aligned}$$

The direction cosines for principal direction 2 are found from the same equations, except that each subscript 1 is replaced by a 2, and similarly for principal direction 3.

The bearing and inclination of any principal stress can be found as follows. It is easily shown that, for direction 1,

$$[\cos(\text{angle of inclination of } S_1)] \times [\cos(\text{bearing of } S_1)] = m_1' \quad \text{(A13)}$$

$$[\cos(\text{angle of inclination of } S_1)] \times [\sin(\text{bearing of } S_1)] = l_1' \quad \text{(A14)}$$

from which

$$\tan(\text{bearing of } S_1) = l_1'/m_1' \quad \text{(A15)}$$

Given the bearing angle, the inclination can be found from equation A13 and A14.

APPENDIX B

DIELECTRIC MATERIALS

RYNITE

by Dupont Canada Inc.

March 1985

841-1251

INTRODUCTION

RYNITE® is DuPont's registered trademark for its thermoplastic polyester resins.

RYNITE thermoplastic polyester resins, listed in Table 1, contain uniformly dispersed glass fibers or mineral/glass fiber combinations in polyethylene terephthalate (PET) resin which has been specially formulated for rapid crystallization during the molding process. RYNITE thermoplastic polyester resins have a unique combination of properties – high strength, stiffness, excellent dimensional stability, outstanding chemical and heat resistance, and good electrical properties.

RYNITE® PET resins are noted for their excellent melt flow characteristics, close molding tolerances, and high productivity from multicavity molds. The properties, processing characteristics, and competitive price of the RYNITE® thermoplastic polyester resins lead to high value-in-use and lower part costs.

TABLE 1/RYNITE® RESINS

GENERAL PURPOSE GRADES

Standard Compositions	Characteristics	Typical Uses
RYNITE® 530	30% glass-reinforced modified polyethylene terephthalate – outstanding balance of strength, stiffness and toughness, good electrical properties, and excellent surface appearance.	Ignition components, coil caps, relay bases, gears, sprockets, carburetor components, various pump housings, vacuum cleaner parts, furniture parts, lamp sockets.
RYNITE® 545	45% glass-reinforced modified polyethylene terepthalate – greater strength and stiffness, excellent dimensional stability and creep resistance.	Lamp housings, compressor housings, fuel, air and temperature sensor housings, frames, filament spools, coil bobbins, transmission components, medical devices.
RYNITE® 555	55% glass-reinforced modified polyethylene terephthalate – superior stiffness, dimensional stability, heat resistance, and outstanding resistance to creep.	Structural support brackets, clamps, structural housings and covers, transmission components, propellors.

LOW WARP GRADES

RYNITE® 935	35% mica/glass reinforced modified polyethylene terephthalate – low warpage, good electrical properties, high stiffness, high heat resistance.	Exterior body parts, structural housings and frames, irrigation components, electrical components.
RYNITE® 940	40% mica/glass-reinforced modified polyethylene terephthalate – greater strength, stiffness and low warpage.	Frames, exterior body parts. Structural supports.
RYNITE® 940 FB	Foam injection molding version of RYNITE® 940 for minimum sinks opposite ribs and bosses.	Frames, exterior body parts.

TABLE 1/RYNITE® RESINS (cont.)

TOUGHENED GRADES

Standard Compositions	Characteristics	Typical Uses
RYNITE® 430	30% glass-reinforced modified polyethylene terephthalate – improved impact resistance – excellent balance of strength, stiffness, and temperature resistance.	Water pump housings, structural housings and brackets, windshield wiper blade supports.
RYNITE® SST 35	35% Stiffened Super Tough glass-reinforced modified polyethylene terephthalate-superior combination of toughness, elongation, stiffness and temperature resistance. Excellent moldability and surface appearance.	Automotive components, wheels, housings, sports equipment, yard and shop tool housings, furniture and luggage components.

FLAME-RETARDED GRADES

RYNITE® FR-530	Flame-retarded, 30% glass reinforced modified polyethylene terephthalate. Recognized by UL as 94 V-O with temperature indexing of 150°C. Outstanding balance of properties and excellent flow characteristics.	Electrical and electronic connectors and other components requiring flame-retarded characteristics. Used in applications employing vapor phase and wave soldering techniques. Also used for high temperature bobbins.
RYNITE® FR-945	Flame retarded, 45% mineral/glass reinforced modified polyethylene terephthalate. Lower cost, lower warpage than FR-530.	Similar to FR-530 but tailored for applications requiring lower cost and warpage.

PROPERTIES

Summary

Typical properties of the RYNITE® resins are listed in Tables 2 and 3.

TABLE 2 TYPICAL PROPERTIES OF RYNITE® THERMOPLASTIC POLYESTER RESINS S.I. UNITS

	Property[1]	ASTM Method	Units	General Purpose RYNITE® 530	General Purpose RYNITE® 545	General Purpose RYNITE® 555	Low Warp RYNITE® 935	Low Warp RYNITE® 940	Toughened RYNITE® 430	Toughened RYNITE® SST-35	Flame Retarded RYNITE® FR-530	Flame Retarded RYNITE® FR-945
STRENGTH	Tensile Strength											
	–40°C	D 638	MPa	218	242	221	121	168	186	196	207	139
	23°C		MPa	158	193	196	96.5	126.3	124	103	152	104
	93°C		MPa	83.2	91.6	95.8	44.1	55.9	44.9	62	86.2	51
	149°C		MPa	56.4	66.8	70.9	30.3	38.6	30.3	46	55.8	31.7
	Elongation at break											
	–40°C	D 638	%	2.5	1.7	1.3	1.8	1.7	3.2	3.5	2.3	1.2
	23°C		%	2.7	2.1	1.6	2.2	1.9	3.2	6.0	2.3	1.4
	93°C		%	5.7	4.5	4.0	4.6	5.5	4.9	10	4.8	3.3
	149°C		%	6.5	6.0	4.5	5.1	6.5	4.9	10	6.5	5.1
	Shear Strength											
	23°C	D 732	MPa	79.2	86.1	82.7	53.7	60.7	58.6	38	65.5	48.3
STIFFNESS & CREEP	Flexural Strength											
	–40°C	D 790	MPa	289	344	358	181	261.5	296.7	276	279	210
	23°C		MPa	231	283	310	148	198	193.2	145	221	154
	93°C		MPa	114	141	165	62	73	69	69	107	95.2
	149°C		MPa	75.8	96.5	110	42.7	49	–	–	68	66.9
	Flexural Modulus											
	–40°C	D 790	MPa	10,335	15,160	20,670	11,715	13,248	9,660	8,970	11,032	14,482
	23°C		MPa	8,960	13,780	17,915	9,645	12,144	7,590	6,900	10,343	11,655
	93°C		MPa	3,580	5,510	9,210	3,370	3,588	2,415	2,484	4,275	4,482
	149°C		MPa	2,690	4,000	5,730	2,205	2,070	–	1,898	2,896	2,896
	Compressive Strength											
	23°F	D 695	MPa	172	179	196	141	175	163.5	81	172	168
	Deformation Under Load											
	27.6 MPa	D 621										
	23°C		%	0.4	0.4	–	–	0.6	0.7	*	0.5	.38
	50°C		%	1.6	1.2	–	–	1.5	2.8	*	1.2	1.20
	Flexural Creep											
	27.6 MPa											
	5000 h	D 2990										
	23°C		%	0.56	0.32	0.19	0.48	–	0.63	*	0.46	*
	60°C		%	1.18	0.70	–	–	–	1.52	*	1.01	*
	125°C		%	1.65	1.14	0.81	2.0	2.1	1.96	*	1.86	*
	Heat Deflection Temp.											
	1.8 MPa	D 648	°C	224	226	229	215	211	210	220	224	200
TOUGHNESS	Izod Impact Strength											
	–40°C	D 256	J/m	96.1	123	–	–	69.4	122.8	160	80.1	42.7
	23°C		J/m	101	117	123	64.1	74.7	138.8	235	85.4	48.1
	Fatigue Endurance											
	@10⁶ Cycles	D 671	MPa	40.7	51.0	53.8	33.1	42.7	34.5	*	41.3	38
THERMAL	Melting Point	D 789	°C	254	254	255	252	250	250	250	254	250
	Coeff. of Linear Thermal Expansion[2]											
	–30 to 50°C	E 228	10^{-4} m/m/°C	3.2	2.4	1.4	2.7	3.8	3.4	4.3	2.5	2
	50 to 80°C		10^{-4} m/m/°C	2.7	2.4	1.1	1.8	2.4	2.0	2.4	2.0	.81
	80 to 160°C		10^{-4} m/m/°C	2.2	1.6	0.7	1.8	2.0	3.2	4.3	1.1	2
	Thermal Conductivity	C-177	W/m.K	0.29	0.32	0.33	0.26	–	0.29	*	0.25	.24

TABLE 2/TYPICAL PROPERTIES OF RYNITE® THERMOPLASTIC POLYESTER RESINS S.I. UNITS (cont.)

	Property[1]	ASTM Method	Units	General Purpose RYNITE[2] 530	General Purpose RYNITE® 545	General Purpose RYNITE® 555	Low Warp RYNITE® 935	Low Warp RYNITE® 940	Toughened RYNITE® 430	Toughened RYNITE® SST 35	Flame Retarded RYNITE® FR-530	Flame Retarded RYNITE® FR-945
ELECTRICAL	Volume Resistivity	D 257	ohm.cm	10^{15}	10^{15}	–	10^{15}	10^{15}	10^{15}	–	10^{15}	10^{15}
	Surface Resistivity	D 257	ohm/Sq	10^{14}	10^{14}	–	10^{14}	10^{14}	10^{13}	–	10^{14}	10^{13}
	Dielectric Strength, Short Time											
	0.8 mm disk @ 23°C	D 149	kV/mm	45.3	42.6	–	–	–	–	–	40.9	36.6
	1.59 mm disk @ 23°C		kV/mm	29.6	28.8	–	–	28.2	27.0	–	25.6	24.2
	3.18 mm disk @ 23°C		kV/mm	21.7	21.3	19.7	22.5	21.5	21.7	21	16.9	17.3
	3.18 mm disk @ 93°C		kV/mm	23.2	22.5	–	–	–	–	–	–	–
	3.18 mm Disk @ 149°C		kV/mm	23.2	21.7	–	–	–	–	–	–	–
	Step by Step 3.18 mm disk @ 23°C		kV/mm	17.3	17.3	–	20.9	19.0	18.7	–	13.8	14.9
	Dielectric Constant											
	10^3 Hz	D 150		3.6	4.0	–	3.8	3.8	3.4	*	3.6	4.1
	10^6 Hz			3.5	3.9	–	3.7	3.7	3.4	*	3.6	4.0
	Dissipation Factor											
	10^3 Hz	D 150		0.005	0.005	–	0.008	0.007	0.006	*	007	009
	10^6 Hz			0.012	0.011	–	0.010	0.015	0.016	*	010	.017
	Arc Resistance	D 495	S	125	126	126	131	–	79	–	117	126
FLAMMABILITY	UL Flammability[2,3]	UL-94		HB	HB	HB	HB	–	HB	*	VO	VO@ 1/32"
	Oxygen Index	D 2863	% O_2	20	20	–	–	–	20.8	–	33	33
	Hot Wire Ignition	UL-746A	S	132	146	151	177	–	173	–	300+	300+
TEMP. INDEX-ING	Electrical	UL-746B	°C	140	140	140	140	–	140	*	150	140
	Mechanical w/Impact		°C	140	140	140	140	–	140	*	150	140
	Mechanical w/o Impact		°C	140	140	140	140	–	140	*	150	140
MISCELLANEOUS	Specific Gravity	D 792		1.56	1.69	1.80	1.58	1.62	1.49	1.51	1.67	1.84
	Water Absorption 24 hr. 73°F (23°C)	D 570	%	0.05	0.04	0.04	0.05	0.05	0.06	0.25	0.05	0.05
	Hardness, Rockwell M	D 785		100	100	105	85	–	82	62	100	92
	Hardness, Rockwell R	D 785		120	120	121	119	118	114	107	120	120
	Coefficient of Friction											
	Against Self	D 1894		0.18	0.17	0.27	0.21	–	–	–	0.18	0.20
	Against Steel			0.17	0.20	0.18	0.19	–	–	–	0.19	0.20
	Taber Abrasion CS-17 Wheel, 1000 g		mg/1000 cycles	30	44	–	–	81	44	–	38	81
	Mold Shrinkage[4] for 1/8" (3.18 mm) Thickness											
	Flow		%	0.2	0.2	0.2	0.4	0.2	0.2	0.22	0.2	0.3
	Transverse		%	0.9	0.8	0.7	0.8	0.7	0.9	0.9	0.9	0.7
	Acid Resistance:	Good at room temperature. Attacked by strong and weak acids at elevated temperatures.										
	Base Resistance:	Good at room temperature. Attacked by strong and weak bases at elevated temperatures.										
	Solvent Resistance:	Excellent resistance to wide variety of fluids such as gasoline, motor oil, transmission fluid, hydrocarbons, and organic solvents. Some absorption by ketones and esters causes plasticization and small dimensional changes.										

[1]These values are for natural color (NC-10) resins only. Colorants or other additives may alter some or all of these properties. The data listed here fall within the normal range of product properties, but they should not be used to establish specification limits nor used alone as the basis of design.

[2]Based on specimens 1/32" (0.8 mm) thick.

[3]This small test does not indicate combustion characteristics under actual fire conditions.

[4]Shrinkage determined on 3" x 5" x 1/8" (76.2 x 127 x 3.18 mm) specimen molded at 200°F (93°C).

[5]Measured in flow direction which is predominantly direction of fiber orientation. Values will be greater in transverse direction.

ARALDITE

by Ciba-Geigy Canada Ltd.

March 1985

841-1251

CIBA–GEIGY

Resins Department

Product Data

Araldite® 507

Low Viscosity Modified Epoxy Resin

General	Araldite 507 is a low viscosity general purpose modified epoxy resin. Systems based on Araldite 507 have excellent mechanical properties and chemical resistance. In addition, Araldite 507 has a very low tendency to crystallize compared to other bisphenol A based epoxy resins.	
Chemical Description	Bisphenol A based epoxy resin modified with cresyl glycidal ether.	
Applications	Adhesives Casting Coatings Flooring Laminating Filament winding Tooling	
Advantages	Low viscosity Very low tendency to crystallize Excellent cured properties Excellent chemical resistance Easier handling	
Typical Properties	Appearance	clear, no contamination
	Epoxy value eq/100 g	0.52-0.54
	Weight per epoxide	185-193
	Viscosity @ 25°C (77°F),cP	500-700
	Color, Gardner	7 max
	Pound per gallon, typical	9.50
	Flash point, closed up	135°C (275°F)

Formulations

Castings	Parts by weight			
	1	2	3	4
Araldite 507	100	100	100	100
Hardener HY 956	25	—	—	—
Triethylene tetramine	—	11	—	—
Hardener HY 840	—	—	50	—
Hardener HT 907	—	—	—	80
Accelerator DY 064	—	—	—	0.5
Viscosity @ 25°C (77°F), cP	700-800	550-650	3,500-3,900	250-350
Pot life, 100g @ 25°C, min	25-30	20-25	450-510	120-140@ 80°C(176°F)
Cure schedule	7 days @ 25°C (77°F)			4 hr @ 80°C (176°F) + 6 hr @ 120°C(248°F)
Cured Properties				
Flexural strength, psi	17,000	11,000	14,000	11,000
Flexural modulus, psi x 10^5	9.7	7.4	5.7	8.5
Impact strength, ft lb/in^2	1.4	1.9	2.8	2.8
Heat deflection temp°C(°F)	60(140)	55(131)	50(122)	90(194)
Dissipation factor, tan @ 60Hz				
@ 20°C (68°F)	0.007	0.015	0.003	0.002
@ 40°C (104°F)	0.020	0.073	0.025	0.002
@ 60°C (140°F)	—	0.09	0.002	0.002
@ 80°C (176°F)	—	—	—	0.007
Dielectric constant				
@ 20°C (68°F)	3.7	4.0	3.2	3.2
@ 40°C (104°F)	4.0	5.4	3.5	3.2
@ 60°C (140°F)	5.3	—	4.2	3.2
@ 80°C (176°F)	—	—	—	3.8
Volume resistivity @ 20°C, cm	10^{16}	10^{15}	10^{16}	10^{17}
Dielectric strength @ 20°C, kV/cm	260	250	280	225

Coating Formulations	1	2	3	4
Araldite 507	100	100	100	100
Hardener HY 2964	50	—	—	—
Hardener HY 2969	—	60	—	—
Hardener HY 837	—	—	35	—
Hardener HY 830/ HY 850	—	—	—	45/15

CIBA-GEIGY

Resins Department

Product Data

Araldite® 502

Low Viscosity Modified Epoxy Resin

General

Araldite 502 is a light colored, medium-low viscosity, modified epoxy resin. It contains a non-reactive diluent, dibutyl phthalate, which increases the resiliency of the cured product and makes it suitable for low temperature applications. Araldite 502 can be crosslinked with amine, anhydride, polyamide and other hardeners commonly used with epoxy resins.

Chemical Description

Liquid epoxy resin based on bisphenol A and epichlorohydrin and modified with dibutyl phthalate.

Applications

- Adhesives
- Castings
- Coatings
- Flooring
- Laminating
- Tooling

Typical Properties

Appearance	clear
Epoxy value, eq/100 g	0.40-0.43
Weight per epoxy	233-250
Viscosity @ 25°C (77°F), Cannon-Fenske, cP	2,100-3,600
Color, Gardner	3 maximum
Pounds per gallon	9.45
Flash point, closed cup, °F (°C)	400 (204)

Formulating

Casting

The following is a typical formulation for casting, potting and encapsulating.

	Parts by Weight
Araldite 502	100
Hardener HY 956	20
Viscosity @ 25°C (77°F), cP	2,000-2,200
Pot life, 100 g @ 25°C (77°F), min	35-45
Minimum cure time, hours	
@ 25°C (77°F)	24
@ 40°C (104°F)	5-7
@ 100°C (212°F)	2-3

Cure Schedule

7 days @ 25°C (77°F) or gel @ 25°C (77°F) + 2 hours @ 100°C

Typical Cured Properties

Tensile strength, psi	8,300
Tensile modulus, psi	3.4×10^5
Flexural strength, psi	14,000
Flexural modulus, psi	4.4×10^5
Compressive strength, psi	16,000
Heat deflection temperature, °C(°F)	63 (145)
Impact strength, ft-lb/in^2	5.6
Elongation, %	7.0
Linear shrinkage, in/in	.0001
Thermal expansion coefficient, in/in/°F x 10^{-6}	90
Thermal conductivity, BTU in/hr ft^2 °F	1.53
Water absorption, 1 hr boil, %	1.1
10 days @ 20°C (68°F), %	0.6
Dielectric constant	
60 Hz @ 25°C (77°F)	4.1
60 Hz @ 60°C (140°F)	5.8
10^6 Hz @ 25°C (77°F)	3.8
Dissipation factor	
60 Hz @ 25°C (77°F)	0.016
60 Hz @ 60°C (140°F)	0.077
10^6 Hz @ 25°C (77°F)	0.020
Volume resistivity, ohm • cm	
@ 25°C (77°F)	0.2×10^{16}
@ 85°C (185°F)	1.2×10^{16}
@ 100°C (212°F)	1.8×10^{10}
@ 149°C (300°F)	2.2×10^8
Dielectric strength, V/10^{-3} in	
60 Hz @ 25°C (77°F)	425

Chemical resistance @ 25°C (77°F)

% Tensile strength retention after immersion time

	30 Days	6 Months	1 Yr	2 Yrs
10% Sodium hydroxide	90.5	79.8	79.5	84.8
10% Acetic acid	23.0	(A)	—	—
10% Sulfuric acid	73.6	62.6	24.7	23.5
10% Hydrochloric acid	80.2	57.3	50.2	30.1
10% Sodium hypochlorite	91.3	81.5	78.5	88.8
Distilled water	84.3	84.3	69.8	74.3
Toluene	41.8	(A)	—	—
Ethanol	18.8	(A)	—	—

(A) test discontinued